A thesis submitted to the Department of Environmental Sciences and Policy of Central European University in partial fulfillment of the Degree of Master of Science

Application of modern technologies for flood exposure analysis- A case study of the Lower Don River basin

Source: Aleksandr Matveev

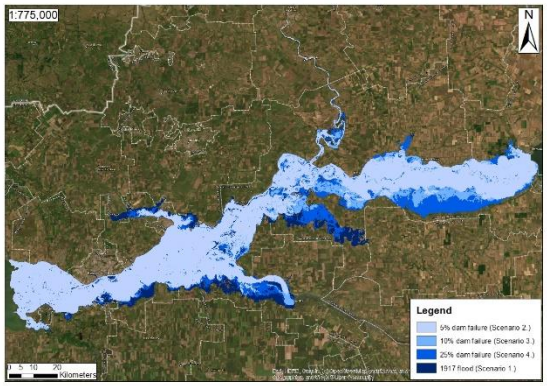

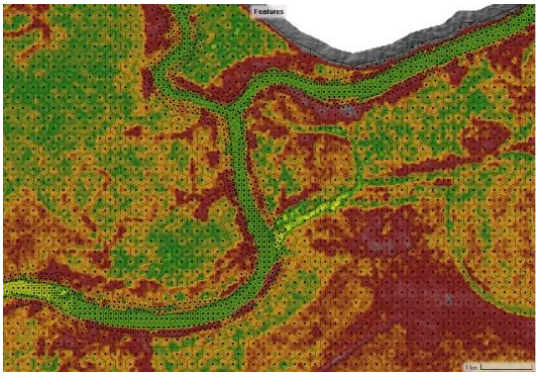

István Attila FILUTÁS

2022 July

Vienna

Notes on copyright and the ownership of intellectual property rights:

(1) Copyright in text of this thesis rests with the Author. Copies (by any process) either in full, or of extracts, may be made only in accordance with instructions given by the Author and lodged in the Central European University Library. Details may be obtained from the Librarian. This page must form part of any such copies made. Further copies (by any process) of copies made in accordance with such instructions may not be made without the permission (in writing) of the Author.

(2) The ownership of any intellectual property rights which may be described in this thesis is vested in the Central European University, subject to any prior agreement to the contrary, and may not be made available for use by third parties without the written permission of the University, which will prescribe the terms and conditions of any such agreement.

(3) For bibliographic and reference purposes this thesis should be referred to as:

Filutás, FI. 2022, Application of modern technologies for flood exposure analysis - A case study of the Lower Don River basin, Master of Science thesis, Environmental Sciences and Policy, Central European University, Vienna

Further information on the conditions under which disclosures and exploitation may take place is available from the Head of the Department of Environmental Sciences and Policy, Central European University.

Author's declaration

No portion of the work referred to in this thesis has been submitted in support of an application for another degree or qualification of this or any other university or another institute of learning.

István FILUTÁS

ABSTRACT OF THESIS submitted by: István Filutás

As climate change, floodplain urbanization continue to cause a greater impact on the environment, global flood risks and hazards are increasing gradually. In order to protect human and material assets, it is important to be able to efficiently analyze environmental processes and their impact on society with the help of developing information and communication technological achievements. Modern remote sensing, geospatial information system and hydraulic modeling technologies provide an opportunity to examine in detail the exposure of a given area to floods. Built up areas are the most vulnerable from land use categories in terms of human life and property value, so the protection of these areas is of key importance. The precise capabilities and use of the mentioned information and communication technologies in the field of exposure assessment of built up areas were presented through the case study of the Lower Don River located in Russia. The amount of water flowing down the river is currently regulated by the Tsimlyansk Dam, which will reach the end of its design life span in the decade of 2020, thereby further increasing the significant flood risk in the downstream region. In this study, the effect of 4 possible flooding scenarios was modeled. Of these, 1. showed the effects of the largest water discharge ever measured on the Don River, and 3 indicated the effects of a possible dam failure on the floodplain. Based on the modeling results, it could be said that the flood exposure of built up areas in many nearby settlements is extreme in terms of water depth. This thesis could be used for multiple purposes. On one hand the methodology described in the study could also be applied in other water systems to investigate flood exposure. On the other hand the results of the case study could be decisive for the bodies responsible for local flood protection and urban development.

Table of Contents

List of Tables

List of Figures

List of Abbreviations

1D	1 dimensional
2D	2 dimensional
3D	3 dimensional
DEM	Digital elevation model
DSM	Digital surface model
DTM	Digital terrain model
EMS	Electromagnetic spectrum
GIS	Geospatial information systems
ICT	Information and communication technology
LIDAR	Light detection and ranging
MASL	Meters above sea level
NASA	National Aeronautics and Space Administration
SRTM	Shuttle Radar Topography Mission
SWAT	Soil & Water Assessment Tool
UNOOSA	The Office of Outer Space Affairs of the United Nations

1. Introduction

The proportion of people at risk of flooding and the critical infrastructure exposed has increased dramatically around the world in recent decades and this trend is expected to continue in the future. In the modern world, floods cause more casualties and economic damage than any other natural disaster. It is enough to think of the recent floods in Europe, China, or Indonesia. The main drivers of the increasing global flood risk are, among other things, the extreme rainfall caused by the intensification of the water cycle accelerated by climate change and the rapid spatial growth of riverine and coastal cities, towns, and industrial facilities. Today, in several countries, regulations require the development of flood risk assessments and measures to manage and reduce flood risks to prevent flooding of vulnerable areas and the occurrence of major material damage. The necessary flood exposure and risk calculations become easier to automate and visualize as modern information and communication technologies (ICT) such as remote sensing, Geospatial Information Systems (GIS), and hydraulic modeling advance.

This study aims to provide a comprehensive summary of the most effective flood mapping technologies available today for exposure analysis and demonstrates their use through a case study. In the case study, riverine floods on the Lower Don River floodplain are simulated and analyzed, which is located in the southwestern part of Russia, between the Tsimlyansk Reservoir and the Sea of Azov deltas. Water flow in the approximately 300 km long target river section is currently controlled artificially by the Tsimlyansk dam, however, extreme weather and heavy rainfall driven by climate change may exceed the dam's retention capacity, which may cause major flooding of inhabited areas in the Lower Don. The study analyses the effects of one historical flood event and 3 dam failure scenarios, which were based on available data from local hydrologic stations.

1.1. Problem statement

The future level of hazards of climate change, urbanization and aging hydraulic structures on the population of floodplains regarding flood safety is not well explored; therefore there is a need for a comprehensive study that discusses technologies for analyzing flood exposure and demonstrates the findings through a case study.

1.2. Research Questions

The main research question, and the narrower sub-questions around which the study is centered are listed below:

Main research question:

"What are recent information and communication technologies, which facilitate effective flood inundation mapping and provide an opportunity for the in-depth analysis of fluvial flood exposure of built-in areas in a given area?"

Sub-questions

- *"What is the level of fluvial flood exposure of built-in areas and under Scenario 1. (1917 historical flood)?"*
- *"What is the level of fluvial flood exposure of built-in areas under Scenario 2. (5% dam failure)?"*
- *"What is the level of fluvial flood exposure of built-in areas under Scenario 3. (10% dam failure)?"*
- *"What is the level of fluvial flood exposure of built-in areas under Scenario 4. (25% dam failure)?"*

1.1. Research objectives

To provide a framework for the research, the following objectives have been formulated:

- Identify efficient modern technologies that facilitate flood exposure analysis.
    - Land-cover mapping
    - Flood inundation mapping
- Determine the fluvial flood exposure of built-in areas in the Lower Don River basin under Scenario 1. (1917 historical flood event)
    - Inundated area (km^2)
    - Water depth (m)
    - Water velocity (m/s)
    - Hazard categories based on water depth and velocity
- Determine the fluvial flood exposure of built-in areas in the Lower Don River basin under Scenario 2. (5% dam failure)
    - Inundated area (km^2)
    - Water depth (m)
    - Water velocity (m/s)
    - Hazard categories based on water depth and velocity
- Determine the fluvial flood exposure of built-in areas in the Lower Don River basin under Scenario 3. (10% dam failure)
    - Inundated area (km^2)
    - Water depth (m)
    - Water velocity (m/s)
    - Hazard categories based on water depth and velocity
- Determine the fluvial flood exposure of built-in areas in the Lower Don River basin under Scenario 4. (25% dam failure)

- Inundated area (km^2)
- Water depth (m)
- Water velocity (m/s)
- Hazard categories based on water depth and velocity

2. Literature Review

2.1. Climate change and flooding in the 21st century

Climate change is a natural process that continuously shifts average atmospheric temperatures and weather patterns and consequently has a significant influence on the world's economy (Stern 2006). 97% of actively publishing climatologists agree on the fact that climate change exists and has a huge impact on the frequency of meteorological, hydrological, and climatological disasters such as floods, storms, landslides, droughts, heat waves, and wildfires (Cook et al. 2016; EM-DAT 2022). Since more and more people are affected by the cascading effects of the global process in recent years increasing attention is being paid to the management of disasters caused by extreme weather events around the world (Mirza 2003; Sikka, Rao, and Rao 2016).

The critical change in average temperature is not a unique phenomenon in the history of the planet. Earth's climate is defined by the succession of climate changes, however, it is important to note that based on the current emissions of greenhouse gases (CO_2, CH_4, H_2O, N_2O) the warming predicted by the end of the 21st century could raise the Earth's temperature to such levels that were unprecedented in the history of mankind (See “Figure 1.”) (NASA 2022).

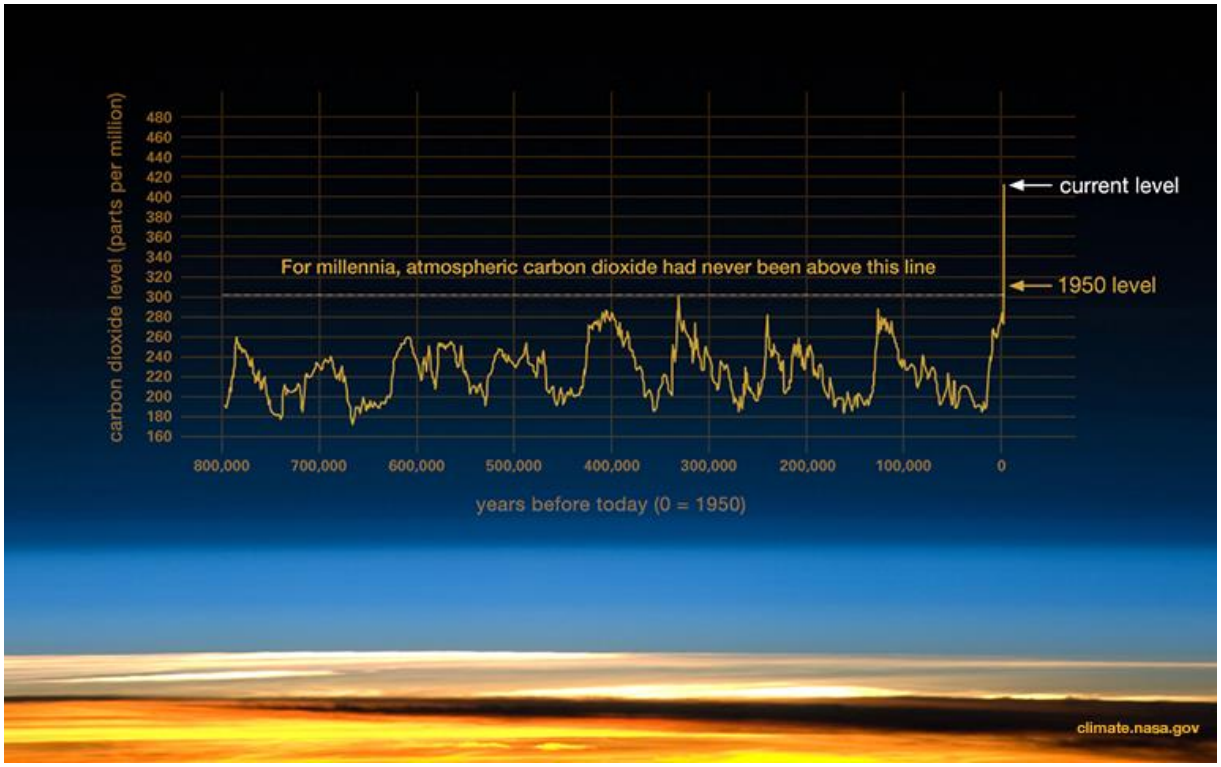

Figure 1.: Present and past atmospheric carbon dioxide concentrations (Source: climate.nasa.gov)

Earth's temperature is changing unevenly in different parts of the world due to the diverse intensity of the greenhouse effect. According to the map of Hawkins of the National Center for Atmospheric Science the arctic and continental regions warm at the most rapid pace while oceanic areas experience milder changes (See "Figure 2.") (Hawkins et al. 2020). In some extreme cases in the North Atlantic, even cooling could be observed due to melted Arctic ice moving southwards with ocean currents but this temporary phenomenon will end as soon as the summer arctic ice permanently disappears. These temperature trends greatly influence the hydrologic cycle and therefore the changes in global precipitation patterns (Hawkins et al. 2020).

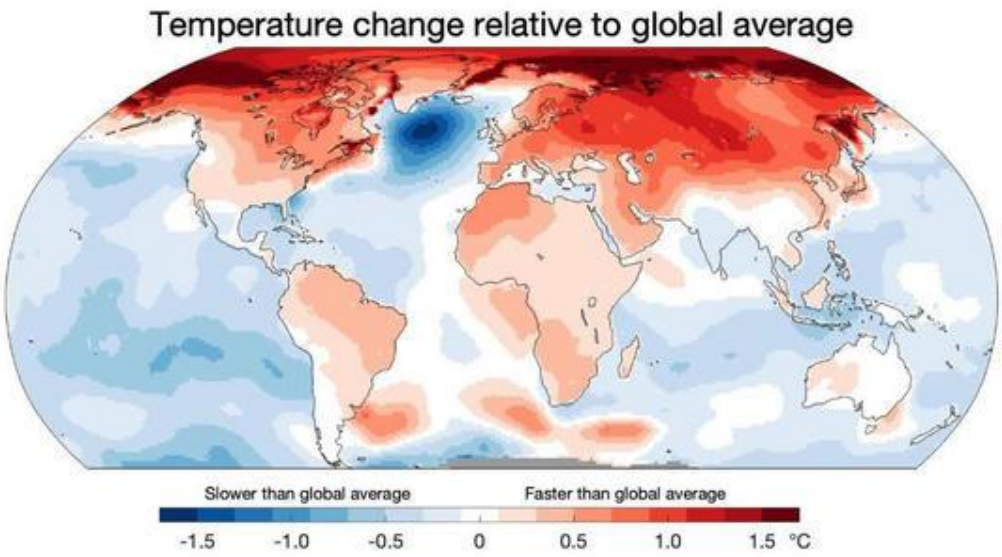

Figure 2.: Temperature change relative to the global average (Source: Professor Ed Hawkins)

The global precipitation change trends are also highly dependent on geographic locations and the timescale of observations (Djebou and Singh 2016). In general, however, it could be said that in those areas, where at present storms are likely to occur the flood risk will increase while less storm-prone areas will experience less rainfall that could lead to extended heat waves and severe droughts (Djebou and Singh 2016).

Due to the extreme weather conditions, the natural processes that trigger floods are also constantly intensifying. Heavy rainfalls are becoming more common as the warming air can hold more water vapor, the average height of storm surge rises as the speed of wind in coastal areas intensifies, and the rapid melting of summer ice in arctic regions and high altitudes result in increasing river discharges (Dore 2005). Floods affect more people and cause more injuries, deaths, economic costs, and damage to the environment and cultural heritage than any other natural disaster (WHO 2022).

In general, floods can be categorized into 2 distinct categories: flash floods and river floods (Australian Government 2022). Flash floods occur within 6 hours of a heavy rainstorm, while river floods take longer to develop. Flood events can be further subdivided into 4 categories

according to their cause: pluvial, fluvial, coastal, and groundwater floods (NOAA 2022). Pluvial floods or occur when the amount of rainwater exceeds the drainage capacity of a certain inhabited area and overflows onto the streets (Rosenzweig et al. 2018). The high-velocity destructive flow can easily sweep cars and poorly constructed buildings away in a relatively short period of time. These floods usually occur in a matter of hours of rainfall, which makes it extremely difficult for responsible bodies and local people to prepare for effective flood defense and damage mitigation (Australian Government 2022). The flood events in Germany and China in July 2021, which caused a total of more than 450 causalities are good examples of disastrous pluvial floods (OCHA 2022; Thieken et al. 2022). The existing drainage infrastructure in the affected regions was not designed to handle such a large quantity of water. Given the high number of causalities and economic damage increasing effort is placed on developing effective flash flood early warning systems (Thieken et al. 2022).

Fluvial floods occur when the water level of a river exceeds the level of the banks and floods onto the floodplain (Australian Government 2022). The accumulation of rainwater runoff in the river takes time (concentration-time) that time could be used to raise awareness of a developing hazard and prepare for defense. According to NASA, the number of people living on floodplains is rapidly increasing (NASA 2021). The globally rising flood risk from fluvial floods is not only a result of the negative effects of climate change but human activity in the form of floodplain urbanization (See “Figure 3.”) (NASA 2021). In ancient times already, people usually established their settlements on the banks of rivers and other water bodies. They grew their plants on the nearby lands because it was easier to extract the necessary amount of water for agriculture and livestock (Rector 2016). In modern times the cities and industrial areas near rivers keep growing, occupying space that is essential for effective flood management. According to a study on the proportion of people exposed to floods, approximately 250-290 million people are living at immediate flood risk. The increase over the

last 2 decades was 56-86 million (Tellman et al. 2021). When a densely built area experiences flooding the extent of the inundation is larger and the duration is longer compared to floods in open spaces due to the lack of room for water (Kaźmierczak and Cavan 2011). Reconciling water management with the basic human needs of the urban population while maintaining urban expansion is an extremely difficult and complex task for municipalities and urban planners (Cocheci 2014). The critical infrastructure along rivers is usually protected with hydraulic structures such as dams or levees. The design lifespan of major infrastructure projects is usually between 50 and 80 years, meaning that most of the critical water infrastructure is already or will soon operate beyond their design life (Union of Concerned Scientists 2022). The maintenance cost of these dams increase gradually and pose increasing threat to those living downstream of the dam due to deterioration of the static condition of the structure (United Nations University 2021). To decrease flood risk on the downstream side of dams these massive structures need to be properly maintained. Maintenance concerns are compounded by the fact that, on a global scale, the resources of river sand that is essential for creating concrete are running low, so these works are expected to become increasingly costly (Bendixen et al. 2019).

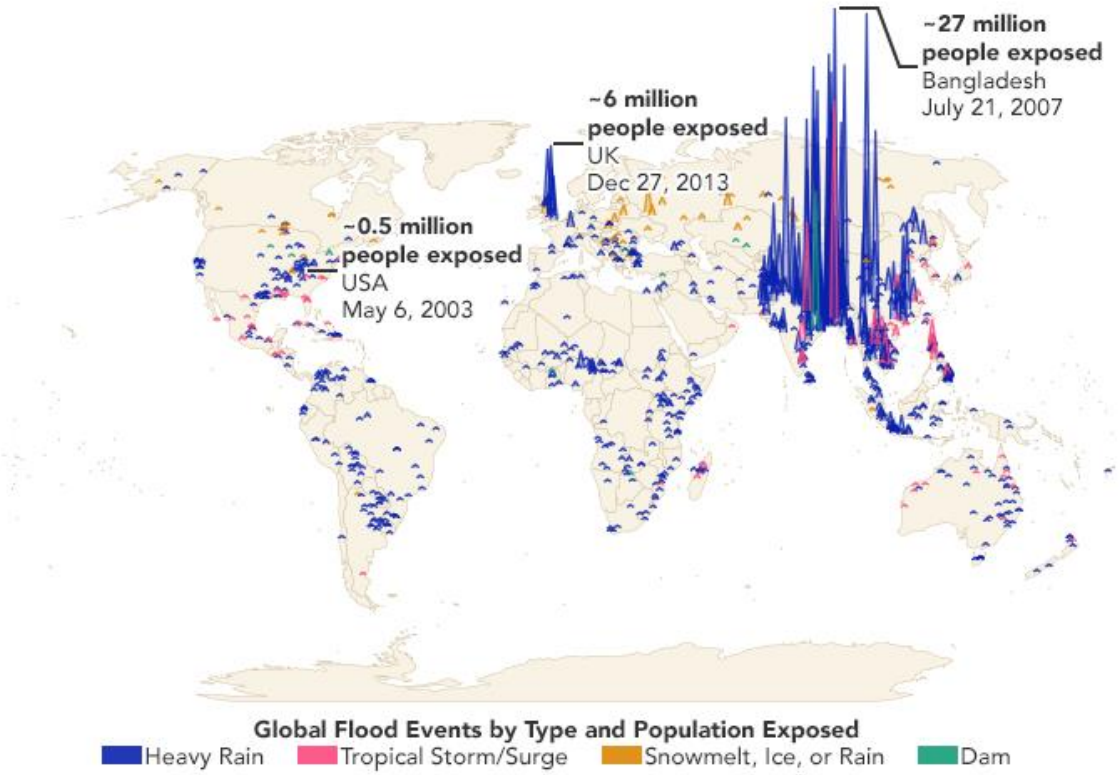

Figure 3.: Global flood events by type and population exposed (Source: NASA)

In 2022 around 2 100 people were affected by the negative effects of fluvial floods in eastern Borneo in Indonesia. The rainfall-runoff that flowed into the Barito River exceeded the river's maximum carrying capacity thereby flooding the homes of locals in the nearby low-lying areas (Davies 2022). The establishment of an effective early warning system, proper coordination of those involved in the flood defense process, and the appropriate design of temporary flood barriers are of key importance when mitigating flood damage from fluvial floods (Kreibich et al. 2015).

Coastal floods are usually associated with low-pressure weather systems such as cyclones (Woodruff, Irish, and Camargo 2013). The main meteorological factor contributing to the storm surge is the high-speed wind that generates destructive waves hitting the shore of a water body. Other factors that affect the severity of storm surges include the shallowness and orientation of the water body and the atmospheric pressure drop of the storm (Mayo and Lin 2022). The

climate change-driven sea-level rise and extreme storms are expected to increase the vulnerability of coastal urban areas to storm surges. For some coastal major cities, such as Jakarta, exposure to rising sea levels and storms may be exacerbated by the overexploitation of groundwater resources (Aldrian 2021). As a result of the extraction of water from underground sources, the soil compresses which leads to the sinking of the ground.

Groundwater or inland floods occur when the level of the underground water table exceeds the ground level submerging houses or other important infrastructure (Australian Government 2022). The determinants of groundwater flood risk contain both natural conditions and human factors. Among the natural conditions elevation and the dominant soil type are notable mentions (Zhang and Schilling 2006). A decisive human factor is land cover, which culminates in improper agricultural and forestry management in rural areas and the urbanization of green spaces in urban areas (Nair and Mirajkar 2021).

2.2. Application of GIS, remote sensing, and hydraulic modeling in flood exposure analysis

At present, the ever-evolving achievements of information and communication technologies are greatly contributing to effective flood management practices around the globe (Vazhacharickal, Raju, and Thomas 2018). The closest related modern ICT technologies are remote sensing, GIS, and hydraulic modeling (Vazhacharickal, Raju, and Thomas 2018). The combination of relevant software allows experts to develop well-functioning flood monitoring, protection, and forecasting systems that ensure a safe and vital environment for the people.

2.2.1. Remote sensing

In general, remote sensing means all sorts of data acquisition procedures that produce data without direct, physical contact with the object under study (Short 2003). Detecting information through some senses of living organisms such as vision, smell, or hearing is also considered remote sensing, however, in scientific literature, this term is mostly used regarding data collection from aircrafts, satellites and drones. The sensors designed by humans cannot only work with the visible part of the electromagnetic spectrum (EMS) but they usually can obtain information also from the infrared, thermal infrared, and microwave regions (Elachi and Zyl 2021). The detection of information by modern satellites through multiple bands makes it possible to do targeted use of the data. With a specific combination of bands remote sensing experts can visualize and analyze data on vegetation, urbanization, surface water, elevation, moisture content of the soil etc. (Elachi and Zyl 2021). The most important feature of space sensing is that it can automatically transmit a relatively large amount of data to the sensors on the ground. The operating satellites scan the earth's surface with a frequency depending on their orbital characteristics. The repeated image detection of the same area allows room for multi-temporal analysis (Ban 2016). Following the appropriate conversion processes, the sensed data can be adapted to GIS. A more detailed description of GIS can be found in Chapter 2.2.2..

Data from satellites could be used to gather information on the extent and dynamics of major flood events. According to The Office of Outer Space Affairs of the United Nations (UNOOSA) Sentinel-2 is the most suitable of all satellites for collecting data for flood mapping and damage assessment (UNOOSA 2022). Using the specific band combination defined for surface water delineation the inundated areas in a historic flood event could be identified (UNOOSA 2022). Unfortunately, in the case of passive remote sensing, a thick cloud cover could easily disable the detection of relevant data, because the electromagnetic waves cannot penetrate clouds (Hoque et al. 2011). This difficulty may be most problematic when examining floods in monsoon countries (Hoque et al. 2011). Another limiting condition is the revisit frequency of satellites. Sentinel and Landsat satellites orbit perpendicular to the equator and have uneven revisit times in different parts of the world (Li and Roy 2017). The number of available satellite images is much higher along the equator than in areas close to the poles (See "Figure 4.").

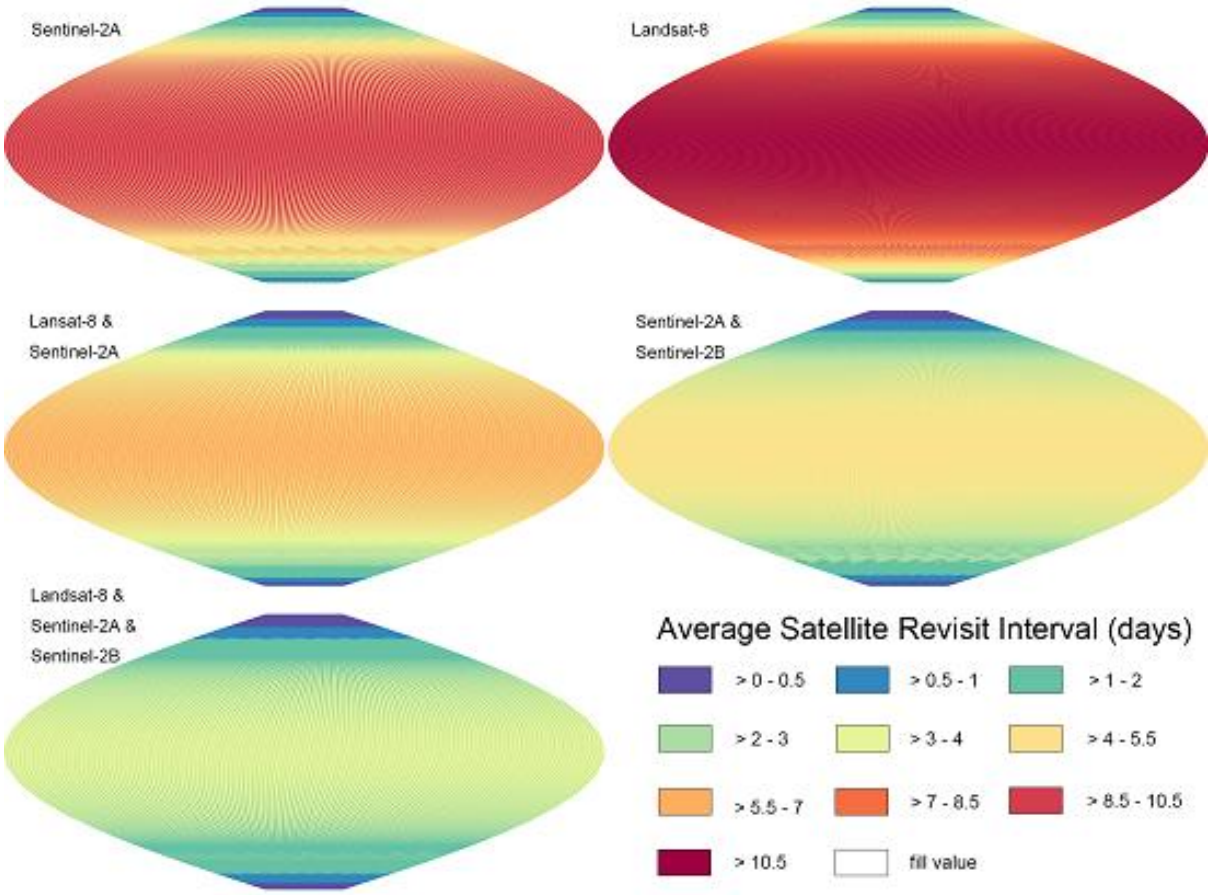

Figure 4.: Global average satellite revisit interval (Source: Jian Li and David P. Roy)

When it comes to flood exposure assessment of a specific region's spatial data on elevation and land-cover is extremely important. Data transmitted from satellites could also be used to develop digital terrain models and land cover datasets. A digital terrain model (DTM) is a digital dataset that stores information on spatial changes of the Earth's surface (European Environment Agency 2022). If this DTM model is supplemented with different surface objects such as vegetation, cars of buildings then it is identified as a digital surface model (DSM) (GISGeography 2016). In flood management, the most common terrain model is the cell-based DTM, which divides the target area into pixels on a basis of a regular rectangular grid (MacOdrum Libary 2022). The position of each cell can be specified by the number of rows and columns, or the coordinates of its center (x; y), and each cell typically contains one value for the area it represents. At present, several companies and organizations are engaged in the

production of global digital terrain models based on radar interferometry with radar signals with a wavelength of a few centimeters (Bashfield and Keim 2011). Of these the Shuttle Radar Topography Mission (SRTM) data produced by NASA is the most widely used with its horizontal resolution of 30 meters (Bashfield and Keim 2011). This DTM is mostly used for flood modeling in regions where data is sparse (Domeneghetti 2016; Yan, Baldassarre, and Solomatine 2013). The production of local, high-quality terrain data is mostly performed by the LIDAR remote sensing method using aircraft or drones (Schumann et al. 2008). The essence of the method is that when measuring the distance between the given point and the instrument, the horizontal and height angles of the laser beam assisting the measurement are recorded by the instrument, so the 3D coordinates of the measured point can be calculated with high accuracy (Wandinger 2005). The point cloud determines the coordinates of millions of points, resulting in a large amount of data (Wandinger 2005).

The negative consequences of floods are significantly affected by land use, as the human vulnerability and material damage varies in different land use categories. For example, if densely populated urban areas are flooded, the economic and social damage is much greater than in the case of floods affecting only arable land. The essential link between land cover and flood management is being increasingly recognised by policy makers (Brody et al. 2014; Zope, Eldho, and Jothiprakash 2017). In 2017, under of the European Union's COST program, the mapping of the relationship between land use and floods began within the framework of LAND4FLOOD, thus helping to prepare more effectively for the growing flood risk. The main objective of the framework is to improve the cooperation between decision makers, land owners, external experts in terms of flood management (Land4Flood 2017). The current accuracy of global land use datasets varies widely. The errors made are usually due to the automation of data generation. Dynamic World, developed by Google and the World Resources Institute is a relatively new (2022) progressive land-use dataset that is updated every 2-5 days

dependent on the exact geographic location of the target area and has a spatial resolution of 10 meters (Brown et al. 2022). The data is derived from Sentinel-2 satellite imagery and is generated by complex machine learning algorithms. The final product could be used for a variety of scientific purposes including flood modeling, urban planning and land-cover change dynamics analysis (Brown et al. 2022).

2.2.2. Geospatial information systems

GIS is an information and communication technology tool that can retrieve information from a database containing data that can be linked to a geographical location. It is used for storing, managing, analyzing and visualizing of digital information that is usually derived from remote sensing datasets. With the spread of networks and online GIS data libraries, the role of accessing and transmitting geospatial information is gaining more and more emphasis globally. GIS appears in different forms in terms of structure and content, in terms of the hardware, software and user environment (Maguire 1991).

The benefits of GIS are most pronounced in complex multi-disciplinary projects like urban planning, emergency management or environmental impact assessments (Parrott and Stutz 1991; Gunasekera 2004). In many cases, spatial decisions need to be made by choosing from a large number of decision pathways based on quantitative or qualitative criteria. GIS software allows the development of organized databases of projects thereby making it easier for decision-makers to evaluate decision alternatives (Bergh 2000).

Geological information and communication technologies are also widely used in flood monitoring, flood risk assessment and post-disaster inundation mapping projects (Shamsi 2022). In Europe the Flood Directive (2007/60/EC) proposed by the European Parliament and of the Council regulates the assessment and management of flood risks in the member countries (European Commission 2007). The directive requires all the member states to develop a preliminary flood risk assessment, hazard and risk maps and protective measures to manage

and reduce the risk of floods. The calculation of hazards and risks and the mapping need to be reported in standardized GIS formats (European Commission 2007) (See “Figure 5.”). Another good example of the benefits of GIS in flood management is the interactive WEB-GIS early warning application in Portugal that was designed to raise awareness of upcoming fluvial floods. With the coupled use of hydrological data obtained from available meteorological weather forecast, GIS software and hydraulic models the program generates expected flood hazard maps for the future, that could be used by acting bodies to prepare for damage mitigation (Mourato et al. 2021).

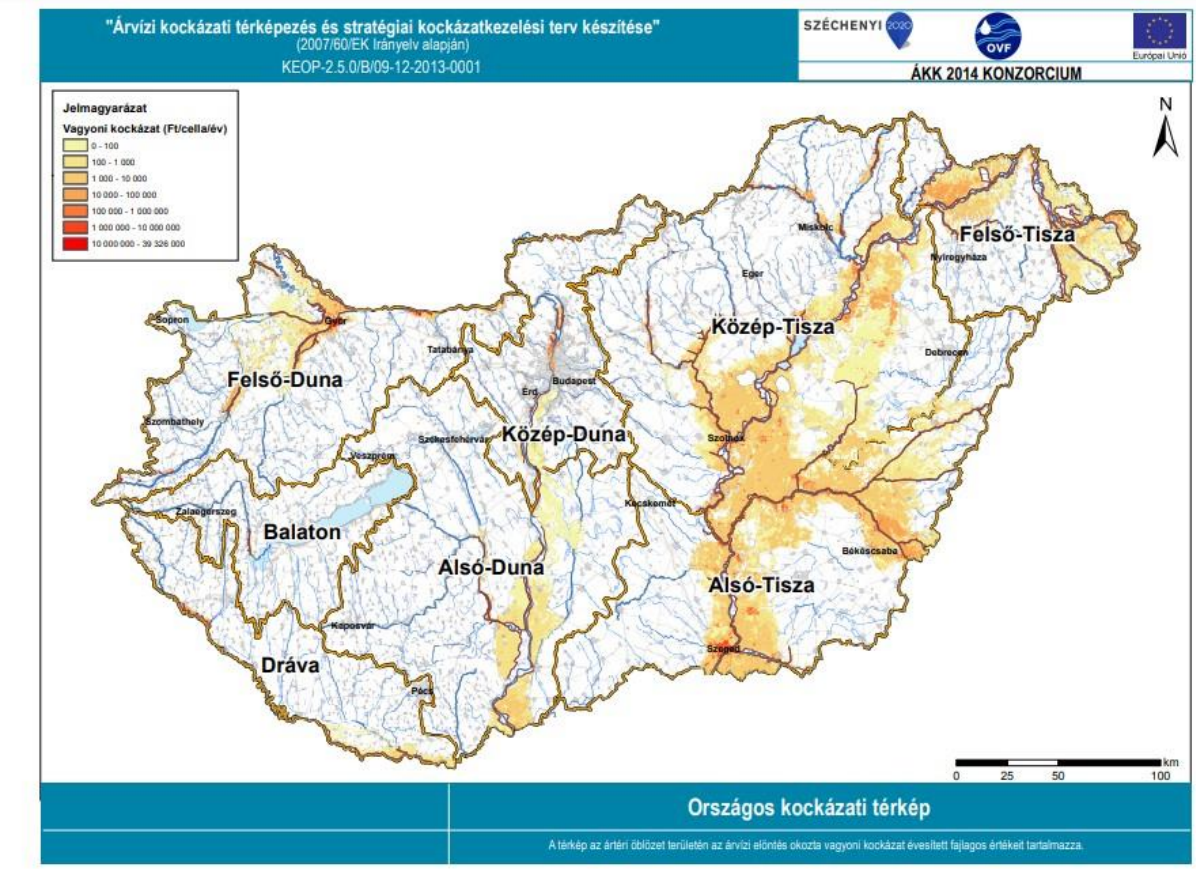

Figure 5.: Flood risk map of Hungary under the EU Floods Directive in 2014. (Source: www.vizugy.hu)

2.2.3. Hydraulic modeling

A hydrological model is usually a digital simplification of a real water system that helps to understand and manage the water resources in a given area. Modern hydraulic modeling software provide an opportunity to study both the qualitative and quantitative properties of water within the water system (Ettema 2000). These models are widely used in the scientific world to estimate flood damage caused by flood events, optimize the use of existing water resources, or investigate the spread and negative effects of potential chemical pollution (Yihdego 2016). When modeling it must be taken into account that models of surface forms and environmental processes can only be considered similar to the real world at an abstract mathematical level. This kind of similarity does not weaken the realistic capabilities of the models in terms of their accuracy and predictions (Ettema 2000).

The concept of "dimensions" often arises in the case of quantitative hydraulic modeling such as the modeling of floods. Dependent on the complexity of the specific flood event and the capabilities of the software used modeling could be carried out in 1D, 2D, and 3D (Morvan et al. 2008) (See “Figure 6.”). 1D models have the simplest geometry and the shortest computation times of all the mentioned types (Hydrologic Engineering Center 2022). They are mostly used when there is only one dominant direction to the flood (usually the centerline of the river), when the large size of the water system under study does not allow for more complex modeling, or when more complex modeling is unnecessary due to the poor quality of available data. Most modeling software use the 1D Saint-Venant equations for water depth calculations (DHI 2021; Hydrologic Engineering Center 2016). 2D models are based on a computational mesh. Each grid contains information on elevation and surface roughness and transmits information to the neighboring cells about the movement of water. The computation mesh allows accurate computation of inundation compared to 1D models when the target river system can be characterized by large flat floodplains, meandering river sections, leveed river

sections or, when flood spreads out in many different directions (Hydrologic Engineering Center 2022). 3D models are the most computation-intensive but they also give the most accurate results of the 3 mentioned types due to their ability to track changes in the spatial distribution of water in all three cardinal directions of space (Vashist and Singh 2021). Such models are severely limited by the size of the target area due to the high computational demands (Vashist and Singh 2021).

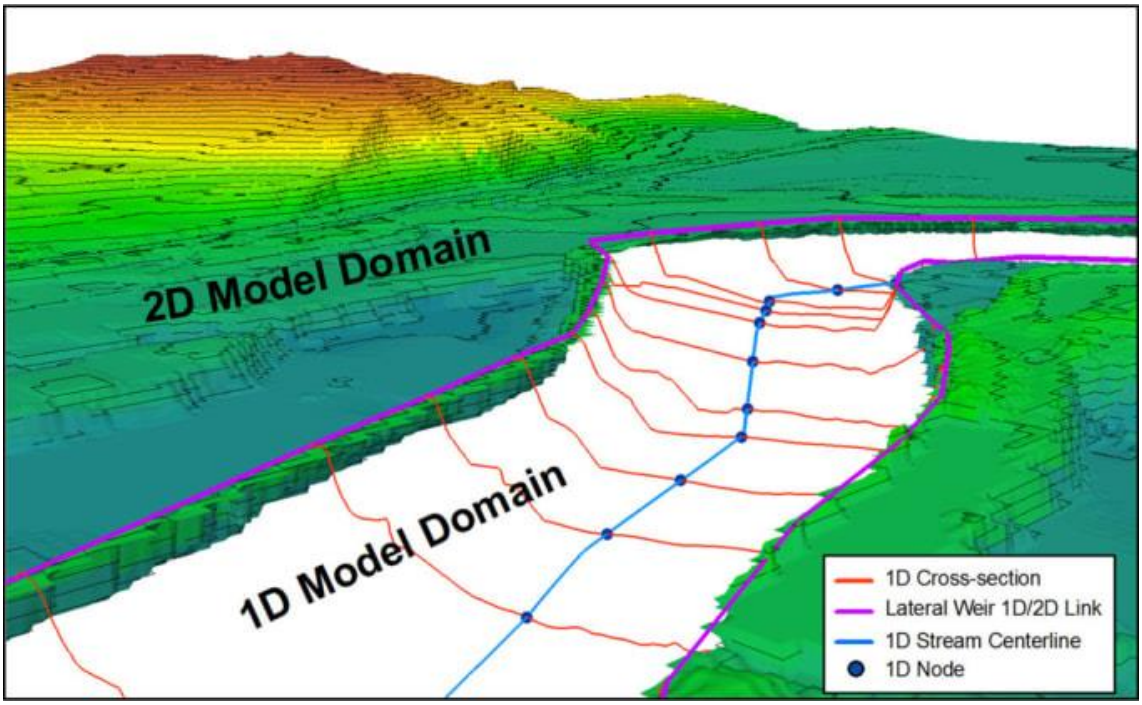

Figure 6.: Difference in the geometry of 1D and 2D hydraulic models (Source: Rodrigo F. Macedo)

As accessing modeling software becoming easier and the accuracy of inundation increases more and more water systems are analyzed in terms of flood risk and more historical flood events are simulated to identify causes and affected areas (Icyimpaye, Abdelbaki, and Mourad 2022; Tamiru and Dinka 2021). A 2022 study by Lee, of the NJ Science Academy aimed at reconstructing the disastrous events of the February 2021 Uttarakhand dam failure in northern India, which counted hundreds of casualties. Based on the calculated arrival times and water depths local authorities could develop an efficient early warning system, and strengthen the disaster resilience of the local communities (Lee 2022).

2.3. Lower Don River- Case study

The modern IT technologies used for flood exposure analysis introduced in previous chapters are presented through the case study of the Lower Don River, which is an approximately 300 km long section of the Don River that reaches from the Tsimlyansk Dam to the Sea of Azov located in the southwestern part of Russia (Gavrilov and Micklin 2022). The following sub-chapters provide detailed information about the hydrological characteristics of the river as well as about its environmental and social background.

2.3.1. Hydrological characteristics of the Lower Don River

The Don River is the 5th longest river in Europe with a total length of approximately 1 870 km (Ruchin et al. 2020). The river rises near Novomoszkovszk and flows through the Caucasus into the Sea of Azov. Based on the physical characteristics and flow patterns of the river it could be divided into 3 sections: Upper Don, Middle Don, and Lower Don (Gavrilov and Micklin 2022). The Lower Don section is located in the middle of a wide valley and thereby has a large floodplain. The main tributaries on the Lower Don section are the Donets and the Manych rivers. The flow of the Lower Don River is controlled artificially with the Tsimlyansk Dam, which is a multipurpose dam that was constructed in the early 1950s (Khetsuriani, Kostyukov, and Ugrovatova 2016) (See "Figure 7."). It allows the artificial flood control of the Lower Don River basin, and generates hydroelectric power. In addition, the retained water is used for irrigation and navigation through the Volga-Don Canal, which is an important shipping route connecting the Volga and Don river basins (European Space Agency 2008). The dam was designed with a life span of 70 years and will operate beyond its design life starting from the beginning of 2023 (Lagutov 2022). To ensure public safety on the Lower Don River floodplain the structure needs to be strengthened.

Figure 7.: Tsimlyansk Dam viewed from the downstream side (Source: imago images/ITAR-TASS)

At present, the average discharge of the Lower Don River section is highly dependent on the available quantity of water in the Tsimlyansk Reservoir. Before the construction of the dam, the flow rate was more variable due to the exposure to natural processes (Rosvodresursy 2013 cited in Kvasha 2014). According to historical hydrological datasets on measured river discharge the average annual flow rate was calculated to be 690 m^3/s before 1952 (Timofeyeva 2008 cited in Kvasha 2014). The highest water levels were usually measured in late spring and early summer when most of the snowmelt water runoff flowed into the river. For the rest of the year, typically low water levels were observed at the measuring stations, which means the population of the floodplain was exposed to seasonal flood risk (Rosvodresursy 2013 cited in Kvasha 2014).

2.3.2. Connectivity between the Lower Don River and populated areas

According to archeological evidence, the first people who settled on the banks of the river lived approximately 40 000-13 000 years ago (Gavrilov and Micklin 2022). These tribes consisted

of only a few hundred members. Since then, the population of the floodplain of the Lower Don River has been continuously increasing, and the area of the natural floodplain has been shrinking proportionally (Gavrilov and Micklin 2022). After the construction of the dam, economic development continued to strengthen. The size of industrial, commercial, and residential areas and other urban infrastructure has increased dramatically. According to a study on the environmental security in watersheds the Lower Don River catchment area is a densely populated and highly important economic region in Russia due to local industry and agriculture (Lagutov, Dronin, and Kirilenko 2010). The total population of the region was calculated to be 4 million in 2000, from which approximately 0,03 % of the population of Russia (World Bank 2022). Most of the local people live in Rostov, which is the capital city of the Rostov Oblast region (ROSSTAT 2013 cited in Kvasha 2014).

The severe effects of climate change could also be observed in the Lower Don River basin. In Russia, the average growth rate of mean annual temperatures was calculated to be double the global average (0.43°C/10 years) (Dzhamalov, Frolova, and Kireeva 2013). Annual precipitation patterns in Russia however do not follow the same trend and have remained nearly constant in the last decades according to measurements. The relative change of the two factors greatly increases the aridity of the region (Lagutov, Dronin, and Kirilenko 2010). Atmospheric warming coupled with increasing rainfall would be beneficial to some extent to the local farmers because warmer temperatures would allow the growing season to be extended. The recent predictions on climate change however suggest that the lack of water for irrigation in case of rainless heatwaves, will cause serious issues for the agriculture sector in the future if no adaptation measures will be applied to boost the efficiency of water resource use (Lagutov, Dronin, and Kirilenko 2010).

The future prediction of Georgievsky and Golvanov on climate change and the quantity of annual river runoff in Russian rivers suggests that the annual total volume of water that flows

down the Don river will decrease by 0-10% (Georgievsky and Golovanov 2019 cited in Gelfan et al. 2022) (See “Figure 8.”). This study however does not present relevant information on the seasonal distribution of total discharges. Despite the annual decrease in the total runoff, the flood risk may stay the same or even increase due to the increasing frequency of extreme weather events. Currently, flood events that result in moderate human and economic damage occur on average once in every 5 years in the Don river basin. Heavy flood events are experienced much less frequently, roughly once in every hundred years (WWF 2008).

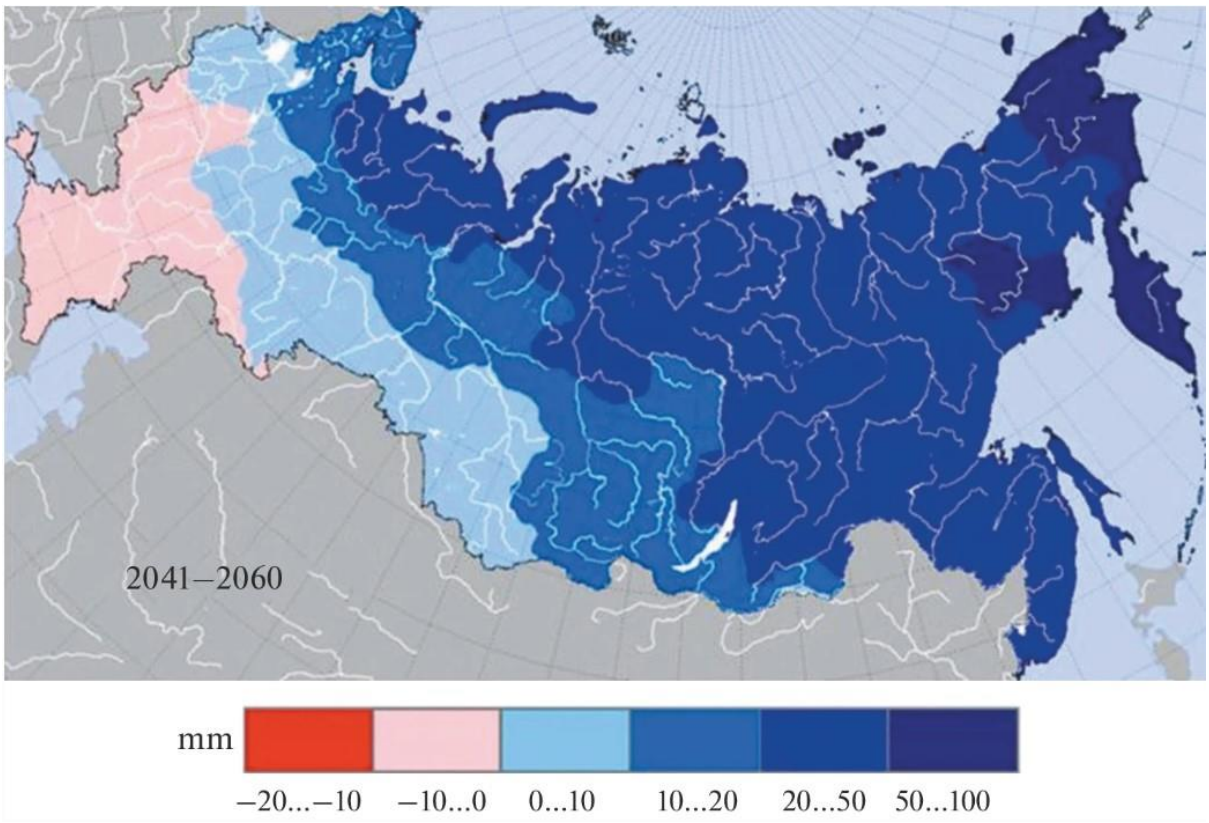

Figure 8.: Possible changes in the mean annual river runoff for the territory of Russia (Source: Georgievsky and Golovanov)

2.3.3. Flood related hazards in the Lower Don river basin

The population of the Lower Don River floodplain is from time to time affected by the primary and secondary effects of storm surge, fluvial and flash floods. In March 2013 the Lower Don River delta was inundated by a strong storm surge affecting 5 300 local citizens (See “Figure 9.”). The reported material damage exceeded 500 000 000 rubles (Matishov et al. 2013). The

highest flow rate ever measured was 14 436 m^3/s on the 23rd of April 1917, before the dam construction near Volgodonszk. The unprecedented amount of river runoff flooded the nearby settlements and caused serious human and economic damages (NPA 2022). Despite the regulated water on the Lower Don River section several historical flood events occurred since 1952. When the water level in the Tsimlyansk Reservoir exceeded the maximum retention capacity for a longer period of time the water was discharged into the Lower Don River causing inundations downstream to the dam. That was necessary to mitigate the possibility of a dam failure, which would cause even greater losses (Rosvodresursy 2013 cited in Kvasha 2014). Establishing operational rules for multipurpose dams is a challenging task, which is made even more difficult by the constantly changing precipitation patterns driven by climate change.

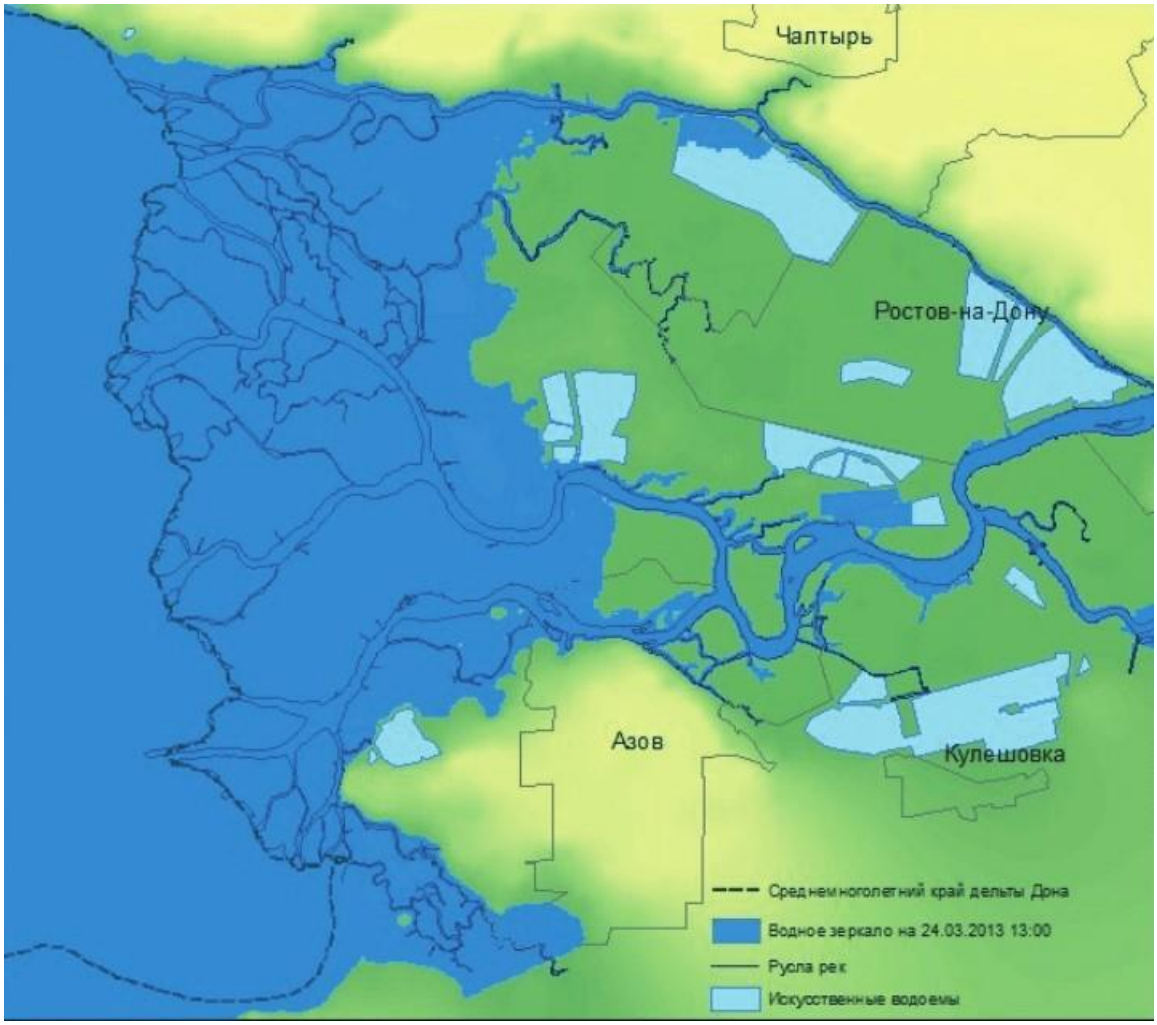

Figure 9.: Flood inundation in the Lower Don delta at 13:00 on March 24, 2013 (Source: Tretyakova and Yaitskaya)

3. Methods

In this chapter, the detailed approach will be described that was used to fulfill predefined research objectives. The methodology of the thesis relied both on literature review and complex geospatial analysis of available data. The main research question was a broader question that could only be answered after gaining a deep insight into the topic by studying relevant literature. The sub-questions, which provided the framework to the case study, however, were answered by applying online remote sensing data processing service, GIS and hydraulic modeling software. The following sub-chapters focus only on the technical approach of the case study and do not describe the process of the literature review.

3.1. Case study workflow

The examination of the exposure of built up areas to various flood events was based on two vital pieces of information. One was the flood inundation area, for the production of which hydraulic modeling was used. The other was land use, that provided information about the environmental and social function of the given area.

For the inundation mapping a HEC-RAS 2D hydraulic model was developed, which was justified by the wide and flat floodplain of the Lower Don River and the risk of backwater floods along the tributaries. The schematic process of creating inundation datasets is shown in Figure 10.. Since all three sub-research questions aimed to investigate exposure based on the current topography and land use conditions, the geometry of the different models was uniform, only their flow and simulation settings differed.

The modelling procedure began with the collection of the necessary data (Step 1.). The data collection process covered geometry data, hydrological datasets on total river discharge, and

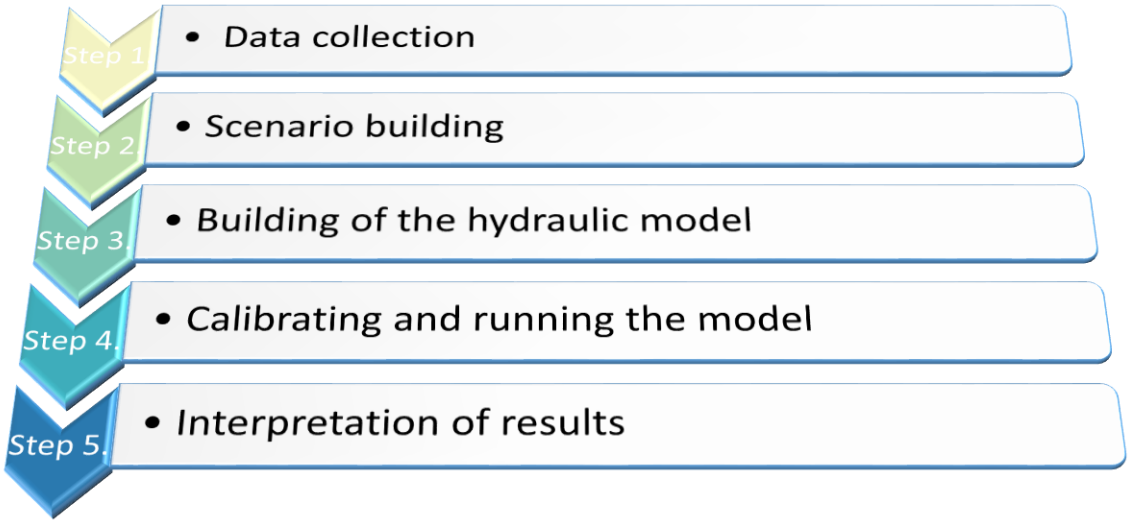

Figure 10.: The schematic workflow of the hydraulic modeling process

the historical inundation maps used for calibrating the model. The properties of the data required for modeling are presented in Table 1.

Table 1.: Data requirement for 2D hydraulic modeling

ID	Data	Geometry/ Flow data/Calibration data	Use	Data type	Remarks
1.	Land-cover	Geometry	Manning coefficient	Shapefile (Polygon)	
2.	Digital Terrain Model	Geometry	Elevation data	Raster	
3.	2D flow area	Geometry	The target area for modeling	Shapefile (Polygon)	
4.	Boundary condition (Don upstream)	Flow data	Don inflow hydrograph (in m^3/s)	ASCII file	
5.	Boundary condition (Donets)	Flow data	Donets inflow hydrograph (in m^3/s)	ASCII file	
6.	Boundary condition (Manych)	Flow data	Manych inflow hydrograph (in m^3/s)	ASCII file	
7.	Boundary condition (Don downstream)	Flow data	Outflow to the Sea of Azov (Water level)	ASCII file	
8.	River centerline	Geometry	Burning stream network into DTM	Shapefile (polyline)	Only needed in case the river bathymetry is not included in the DTM.
9.	Cross-sections	Geometry	Burning stream network into DTM	Any format	Only needed in case the river bathymetry is not included in the DTM.
10.	Historical flood inundation data	Calibration data	Calibrating the model based on historical maps	Shapefile (polyline)	

Scenario building was the second step, during which the exact inflow flow rates and the properties of the outflow section were determined. These scenarios determined exactly where and in what quantity the water enters and leaves the model area. After that, the model was built, which consisted of the generation of the computational mesh, the assignment of elevation values and Manning roughness coefficients data to the cells in the mesh, filling in the data tables of the boundary conditions, and the finalization of the simulation settings. After the initial simulation, the model was planned to be calibrated based on available historical inundation maps by modifying Manning roughness coefficients. The final step was the projection of the finalized inundation maps onto land-use, which provided the opportunity to statistically examine the flood exposure of built-up areas.

3.1.1. Data collection

The data presented in Table 1. were obtained through a number of sources. Google Dynamic World land use data was downloaded from the Google Earth Engine online remote sensing processing application by using export algorithms. Topography data was collected from NASA's online SRTM database. Since the Lower Don River basin is a relatively data sparse area in terms of GIS, the global SRTM topography data with a resolution of 30 m was the most suitable available for modeling. The delineation of the target area (Lower Don River floodplain) was carried out using ArcGIS 10 software, based on SRTM elevation data. The geospatial algorithm delineated the contiguous area in the Lower Don River watershed that did not reach a height of 25 m measured from the riverbed. Flow data input was obtained partly from the database of a previous master thesis (Gilfanova I. 2012– Application of SWAT modelling for assessment of ecosystem goods and services in the Azov Sea basin. Master of Science thesis, Central European University, Budapest.) and partly from the text of the official policy on water resources regulation of the Tsimlyansk reservoir. Unfortunately, the geospatial data required for burning the riverbed into the terrain and the inundation maps required for

calibrating the models were not available, so they were not taken into account in the modeling. The effect of the lack of data on the modeling results is discussed in detail in Chapter 6.

3.1.2. Scenario building

The case study focuses on the analysis of the exposure of built-up areas under 4 different flood scenarios. The first scenario aimed to reproduce the inundation area of the 1917 historical flood event based on the measured maximum discharge (14 436 m^3/s). Such an event could be triggered in the future by climate change. Due to the intense urbanization of the Lower Don River floodplain, this event was expected to affect numerous settlements along the river. The dynamics of the Don River inflow hydrograph was developed according to historical datasets on the daily maximum flow rate at the Razdorskaya measuring station (See "Figure 11."). To mitigate the effects of numerical instabilities due to extreme differences in discharge, a relatively low flow rate was set for the first time steps of the simulation time, and then was gradually increased until it reached the initial value of the flood wave curve. The start time of the simulation was standardized for all the models (June 17th 2022). The first scenario modeled a period of 112 days in order to be able to examine the propagation of the flood wave in its entirety. To include the effect of river runoff from tributaries (Donets and Manych) two additional constant inflow boundary conditions (average flow rate) were added to the model's geometry. The downstream boundary condition was set to sea level, which means that water leaves the 2D flow area as soon as it drops below 0 MASL along the geometry of the boundary condition.

Figure 11.: Don River inflow hydrograph for Scenario 1. (1917 historical flood event)

The other two scenarios aimed to analyze flood exposure in the case of a possible dam failure caused by intolerable pressure from the reservoir. Dam breaks could be caused by the combined effect of the increasing pressure from the upstream side due to climate change and the weakening of the structure's resistance as a result of aging. Firstly, a 5% then a 10% and a 25% dam failure was simulated. The percentage indicate the quantity of water stored in the reservoir. Since no information was found about the bathymetry and storage capacity curve of the reservoir the simulations were based on the total storage capacity value (28.7 km^3). Inaccuracies resulting from lack of data are covered in detail in Chapter 6.. The dynamics of the Don River inflow hydrographs were set to a quasi-permanent condition, which means the excess water flows through the dam during a predefined period of time (24 hours) (See "Figure 12."). The settings of the other boundary conditions remained unchanged compared to the first scenario.

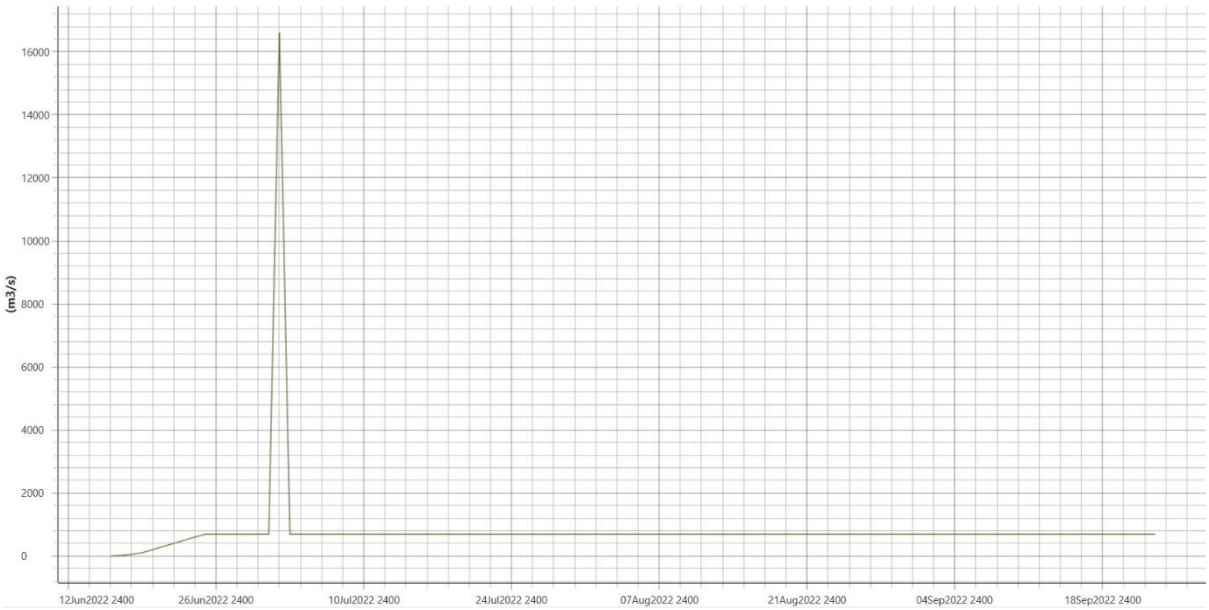

Figure 12.: Don River inflow hydrograph for Scenario 2. (5% dam failure)

3.1.3. Model building and flood inundation mapping

After collecting all the necessary data for modeling and defining the scenarios, the geometry of the HEC-RAS hydraulic model was built. The first step of the process was to define the suitable projection for the target area. Based on to the geographical location of the Lower Don River basin, the "Pulkovo 1995 3 Degree GK CM 39E" projection was determined be the most suitable. After that, the SRTM topography model and the Dynamic World land use data were clipped with 2D flow area polygon and were imported into the model. The roughness coefficient values assigned to different land use categories were determined based on the Harris County Flood Control District HEC-RAS 2D modeling guideline. Table 2. discusses the exact values used for the calculations (Harris County Flood Control District 2019).

Table 2.: The Manning roughness coefficient values (n) used for modeling

ID	Name	ManningsN
0	NoData	0.06
1	crops	0.17
2	trees	0.25
3	shrub	0.25
4	grass	0.22
5	built	0.18
6	flooded_vegetation	0.05
7	water	0.02
8	bare	0.03
9	snow and ice	0.03

After finalizing the terrain and Manning datasets, the computational mesh was generated in the extent of the 2D flow area. The mesh was refined along the flowpaths of the main watercourses, because these are the most critical areas in terms of water level calculations. Misadjusted cell alignment could cause inundation inaccuracies. If the borderline of the cells does not follow the topography patterns, flooding may appear on the floodplain before the water level of the river reaches the elevation of the banks. In the areas further away from the riverbeds, the cell size was set to 200*200 m, because a smaller cell size would have drastically extended the time required for the simulations. The floodplain was covered with hexagon-shaped cells, which provided an opportunity for a more complex examination of the dynamics of inundation, because compared to the traditional square-shaped mesh, water could move in the direction of two more adjacent cells (See “Figure 13.”). When all the mesh editing tasks were completed, cells with more than 8 sides were manually corrected, because these cause errors in HEC-RAS. After the mesh correction finalization, the geometry of the boundary condition lines was inserted. These lines defined the exact locations where the water enters and exits to 2D flow

area. The last steps of the model building process were the integration of the previously developed flow hydrographs and the finalization of the simulation settings.

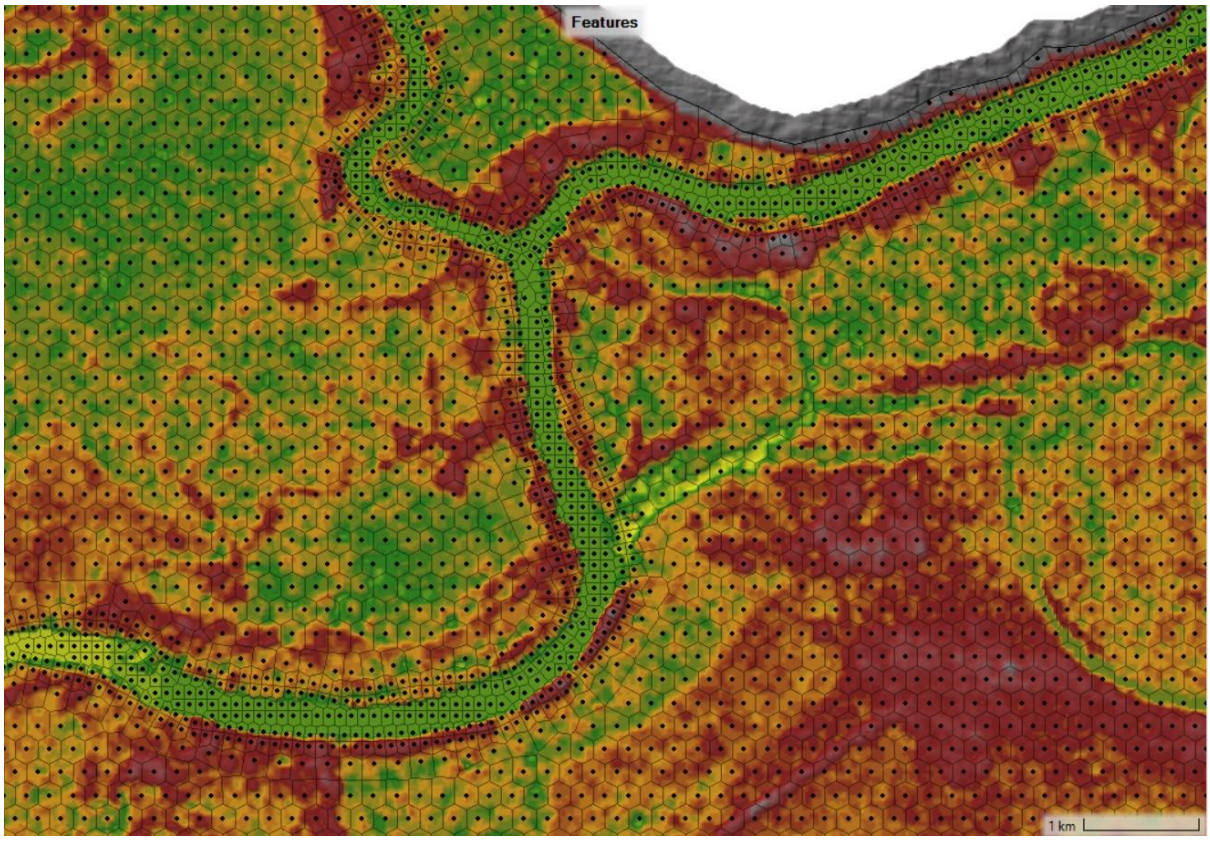

Figure 13.: The final mesh generated for the 2D flow area. The floodplain is covered with hexagon-shaped cells. The mesh was refined along the flowpaths of the main watercourses

3.1.4. Analysis of flood exposure

The finalized inundation and land use datasets allowed the statistical analysis of the exposure of built up areas to flooding. The process of the geospatial analysis was performed using ArcGIS 10 software. Firstly, the total size of the inundation and the affected built up area was calculated, and the flooded areas were classified into flood hazard categories based on maximum water depth and water velocity for all 4 scenarios. Table 3. summarizes the water depth and water speed threshold values for the flood hazard categories. In the case of the dam failure scenarios (Scenario 2, Scenario 3, Scenario 4), in addition to the exposure and hazard

calculations the dynamics of the flood propagation was also investigated, because that provides vital information for local bodies responsible for flood protection.

Table 3.: Flood hazard classification based on water depth and velocity (Source: Ahmed N. A. Hamdan, Abdulhassain A. Abbas)

Hazard Index	Hazard classification	Depth (m)	Velocity (m/s)
1	Very low	≤ 0.5	≤ 0.2
2	Low	0.5-1.0	0.2-0.5
3	Moderate	1.0-1.5	0.5-1.0
4	High	>1.5	>1.0

4. Results

This chapter discusses the results of the flood exposure analysis of built-up areas in the Lower Don River basin. All the data required for the analysis was acquired by using modern remote sensing applications and GIS and hydraulic modeling software.

4.1. Flood exposure results of the 1917 historical flood event

According to the results of the modeling, an event similar to the 1917 flood would cause an unprecedented destruction on the Lower Don River floodplain taking into account current land use patterns. The flood inundation covered roughly 44% of the 9 719 km^2 large model area and 42% of all the built up area located on the floodplain. The maximum extent of the flooding is presented in its entirety in Figure 14.. Several settlements, such as Nikolaevskaya, Romanovskaya, Bagoyavlenskaya, Vislyi, Krivyanskaya, Bagaevskaya, as well as smaller built-up areas located in the river delta were completely flooded and cut off from the outside world. A large part of the city of Bataysk was also inundated, endangering the safety of tens of thousands of people. Of course, effective local protection, which was not taken into account in the current flood mapping could greatly influence the extent of the actual extent of flooding. The effect of the flood could also be observed on the tributaries. On the Donets, the effects of backwater reached up to 77 km upstream from the mouth of the river. In the case of the Manych River the rising water levels were measured up to the Proletarsk Dam located on the border of the 2D model area.

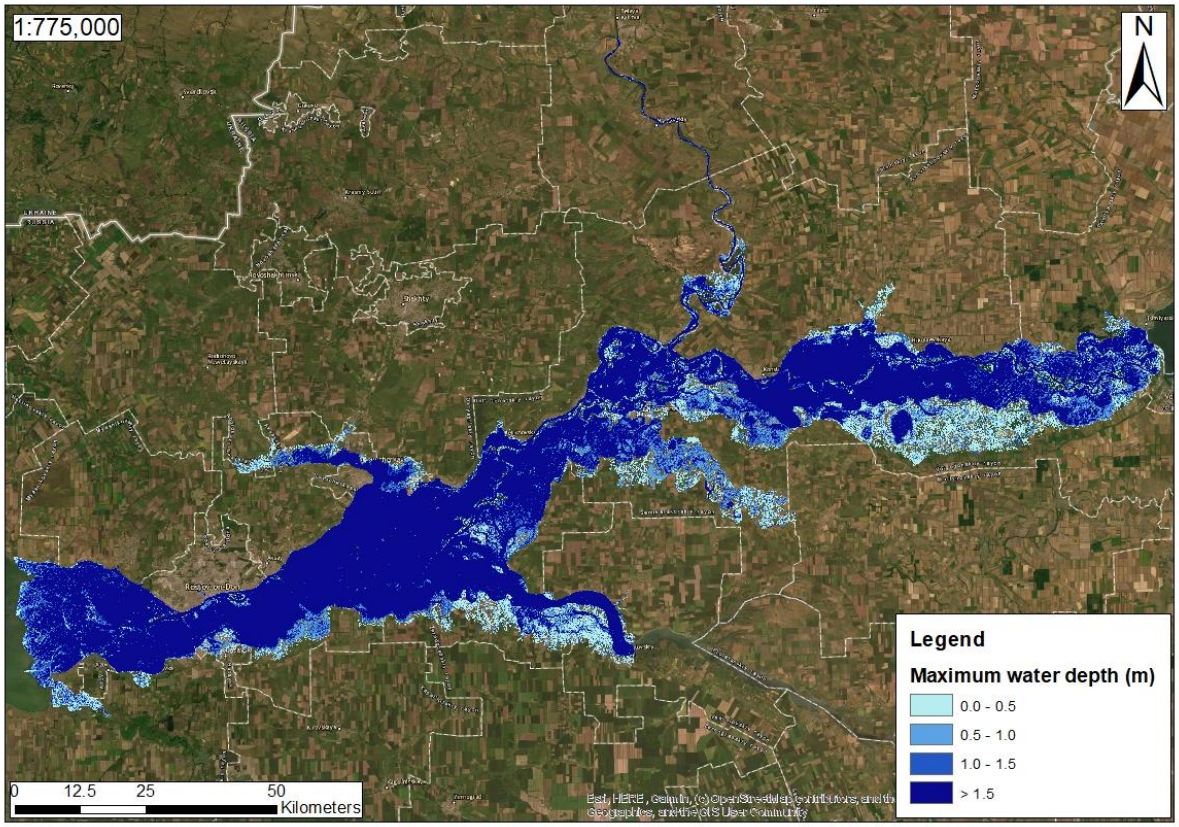

Figure 14.: Maximum water depth results of the 1917 historical flood simulation

Table 4. presents the numerical results of the hazard calculations. Based on the data, it can be concluded that in most of the cases the hazard is considered to be high (79%), which is mainly due to the extreme water depths (See “Figure 15.”). The water depth of several meters can be a particularly big challenge for the bodies responsible for protection to ensure the safety of the exposed population and mitigate the damage of potentially submerged material value. The walls of poorly constructed buildings are highly vulnerable to pressure from deep water and could be damaged or in the worst case scenario, collapse if the exposure lasts for an extended period of time.

Table 4.: The total size of built-up areas according to the different hazard categories for the 1917 historical flood event (Maximum inundation)

Hazard Index	Hazard classification	Total area (km^2)
1	Very low	15.79
2	Low	13.75
3	Moderate	18.07
4	High	178.97
Total		226.57

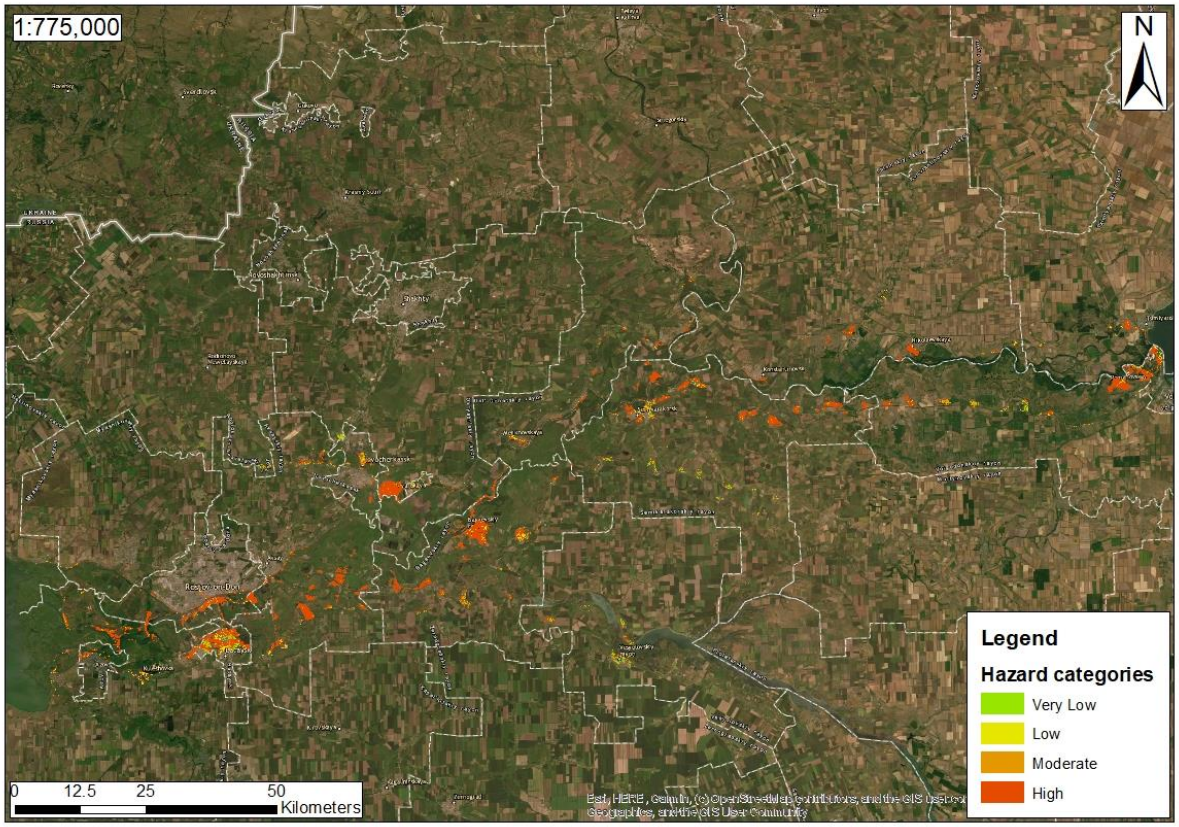

Figure 15.: Flooded built up areas categorized by flood hazard (1917 historical flood event)

In order to gain a deeper insight into the predicted effects of long-term exposure, the flood hazard calculations were repeated for the last time step of the simulation. The last time step was 64 days after the peak of the flood wave, when the water flow rate of the Don dropped below 4 000 m^3/s. At the moment of the last time step of the simulation, 38% of the floodplain was submerged, which means an approximately 576 km^2 decrease in flood extent compared to the maximum inundation (See "Table 5."). The exposure of built up areas has also eased, both in terms of coverage and hazard categories. The total size of highly hazardous areas decreased by 101 km^2, while the extent of less hazardous areas increased roughly equally. Flood hazards clearly decreased in most of the affected settlements, however in the case of some specific built up areas the hazard of flooding remained high throughout the entirety of the simulation (See "Figure 16."). A good example of this is the suburban space located on the southwestern border of the city of Rostov-On-Don, where the high level of hazard stagnated even 63 days after the start of the flood wave receding (See "Figure 16.").

Table 5.: The total size of built-up areas according to the different hazard categories for the 1917 historical flood event (Final time step)

Hazard Index	Hazard classification	Total area (km^2)
1	Very low	39.92
2	Low	33.09
3	Moderate	38.73
4	High	77.82
Total		189.54

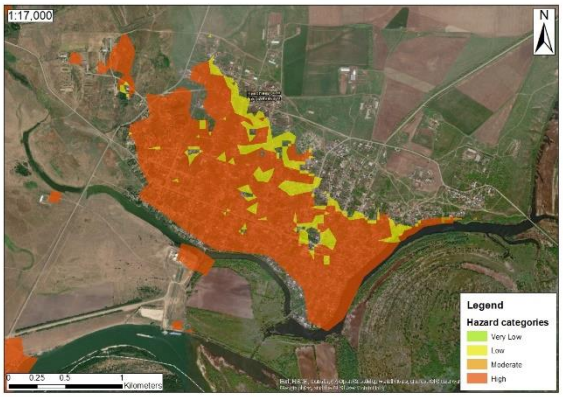

Nikolaevskaya (maximum indundation)

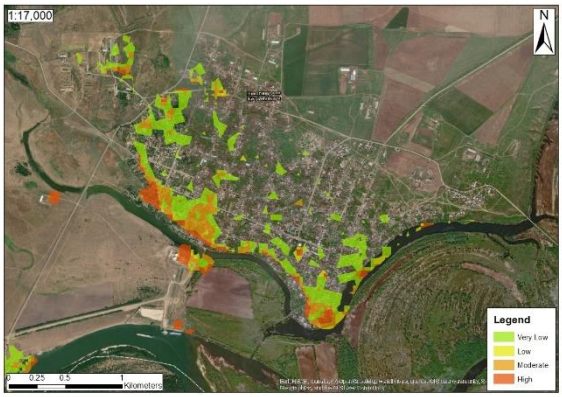

Nikoaevskaya (final time step)

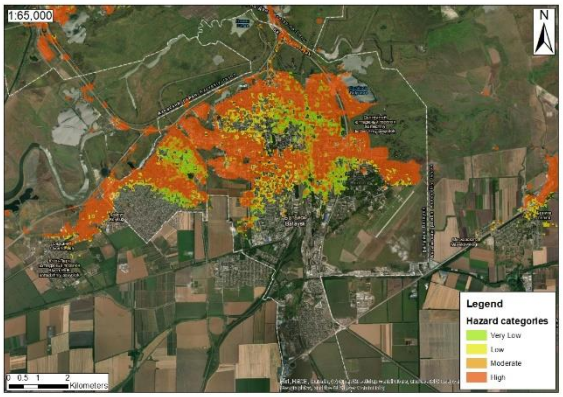

Bataysk (maximum indundation)

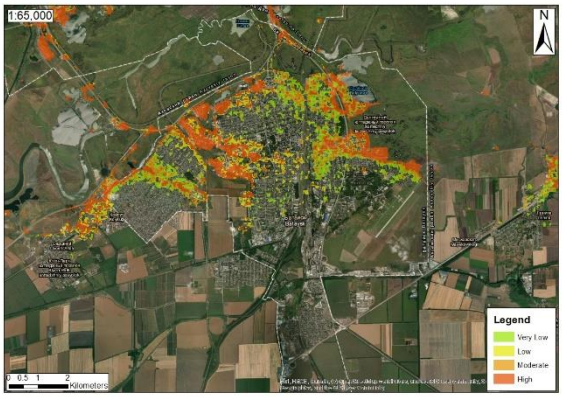

Bataysk (final time step)

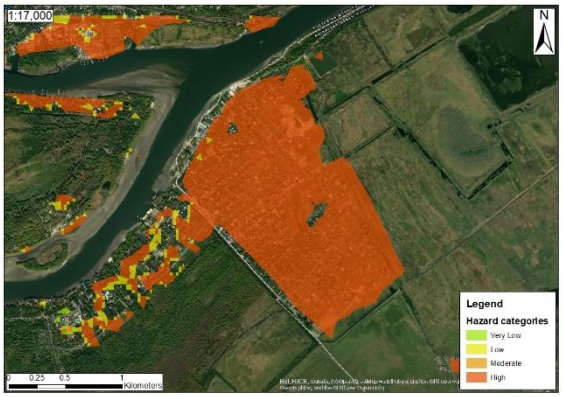

Rostov-On-Don (maximum indundation)

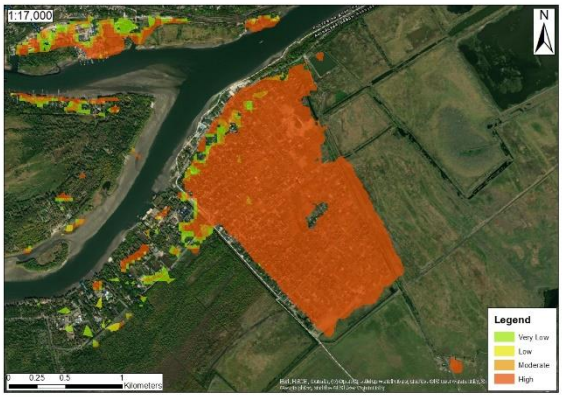

Rostov-On-Don (final time step)

Figure 16.: Changes in local flood hazard at the time of the peak of the flood wave and the end of the retention period

Regarding the results of the flood modeling, it is important to note that the actual receding of the historical flood wave of 1917 most likely occurred faster than it was simulated, because the total quantity of water entering the model area was presumably not that extremely high. The data used to generate the flood wave hydrograph were based on daily measurements and referred to an event with a higher probability, where the maximum flow rate of the Don was only 2 150 m^3/s. As a result of the simple projection of the higher discharge data onto the real flood wave hydrograph, a total quantity of 62.8 km^2 of water flowed into the 2D model area through the Don boundary condition during the 112 day simulation time, which is equal to 2.37 times the average water volume of the Tsimlyansk reservoir. During the simulation, the inflow discharge never dropped below 4 000 m^3/s, so the receding of the flood took place extremely slowly.

4.2. Flood exposure results of the 5% dam failure event

The results of the 5% dam failure showed the lowest water depths, velocities and the lowest flood hazards of all the simulations. Nonetheless, the expected flood damage cannot be neglected. The maximum flow rate calculated at the location of the dam was 16 609 m^3/s, which remained unchanged for a total of 24 hours. The generated inundation was 2 525 km^2 covering roughly 26% of the floodplain. The average water depth exceeded 2 m (See “Figure 17.”). The highest water velocities were observed near the dam, right after the start of the water release from the reservoir. In this region water velocity of 1 m/s could be measured in certain areas, which represents a particularly high risk to human life and the exposed material value, especially when coupled with large water depths. The northwestern suburban areas of Volgodonsk were also exposed to high water velocity (See “Figure 18.”). Flood water entered this area mainly through the Don side-branch in the northern part of the settlement, which enables shipping between the Tsimlyansk reservoir and the Lower Don River (See “Figure 18”). Based on the digital terrain model and relevant satellite images, this branch does not have

flood protection embankments, so the level of the lowest lying points of the bank were already exceeded by the water level in the channel a few hours after the dam break. As a result, defense options may be severely limited following a possible dam failure. In addition to Volgodonsk, rapid and hazardous flooding was also observed in other nearby settlements. Much of Krasnoyarskaya and Romanovskaya, were quickly submerged. The amount of backwater measured on the tributaries was not significant, in contrast to the results of 1917, which was due to the fact that the flood wave quickly receded.

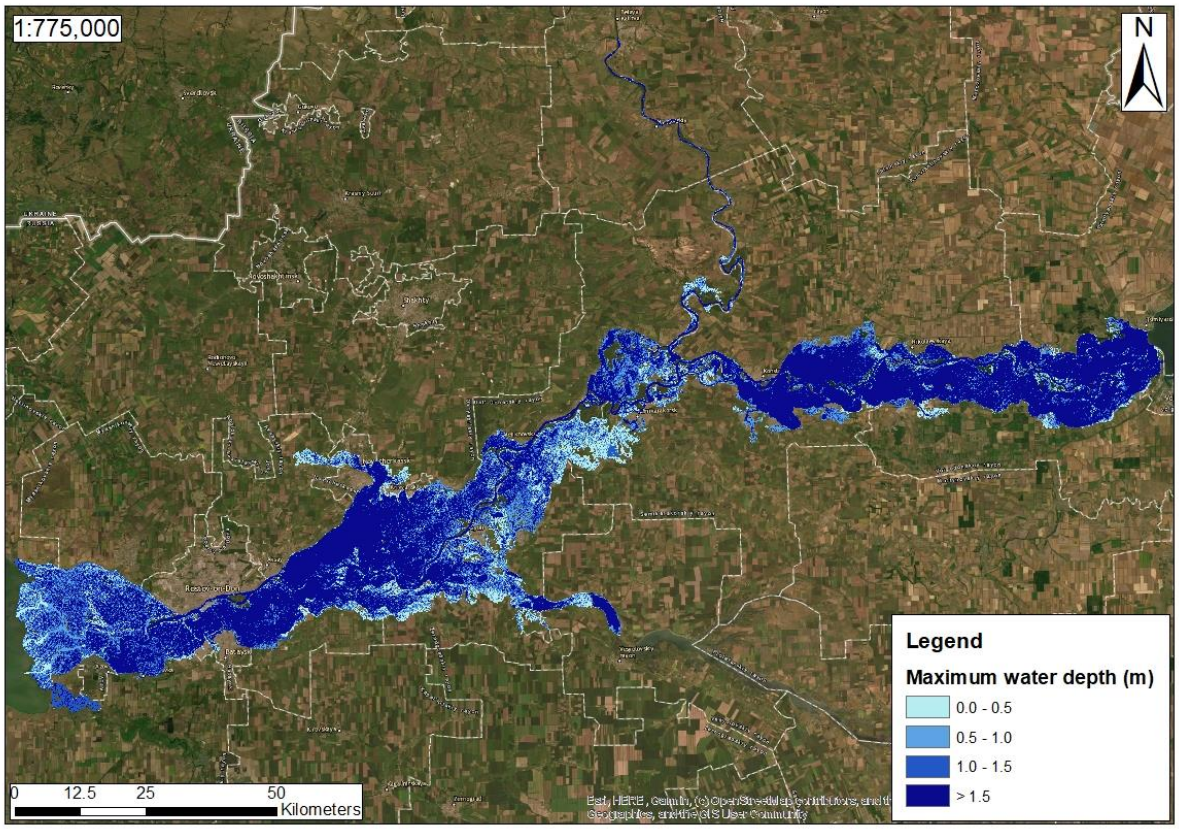

Figure 17.: Maximum water depth results of the 5% dam failure simulation

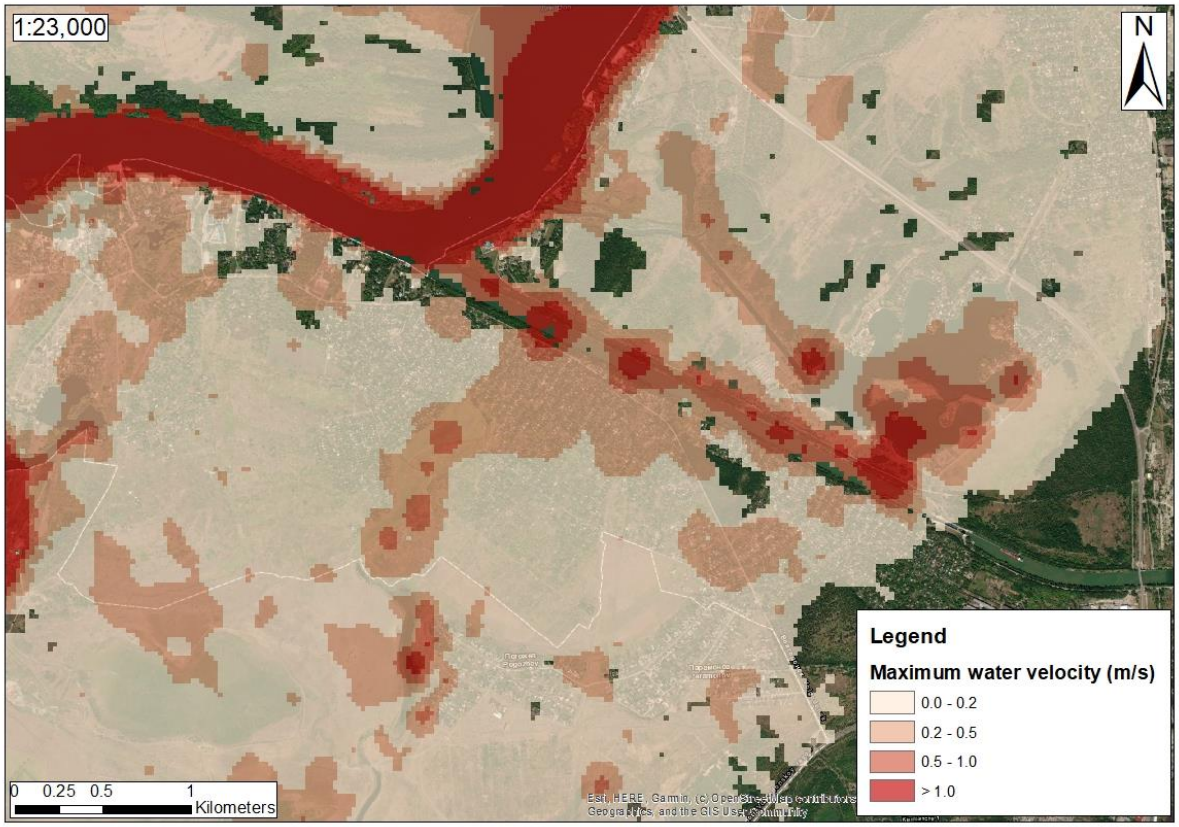

Figure 18.: Maximum water velocity results of the 5% dam failure simulation at Volgodonsk

Based on the inundation results, a 5% dam failure event would cause flooding on a total area of 67.32 km^2, most of which would have a high level of flood hazard (See "Table 6."). The reason for the high level of hazard differs in different parts of the floodplain. In the upstream regions, near the dam, high velocities are responsible for the hazard while further away it is mostly due to extreme water depths.

Table 6.: The total size of built-up areas according to the different hazard categories for the 5% dam failure simulation

Hazard Index	Hazard classification	Total area (km^2)
1	Very low	14.17
2	Low	8.49
3	Moderate	12.46
4	High	32.20
Total		67.32

The effect of the flood wave coming from the direction of the dam could be detected approximately 14 days after the event along the downstream boundary condition. The relatively slow flood propagation of the flood wave can provide an opportunity to develop an effective temporary defense strategy in vulnerable settlements further away from the dam, such as Ol'ginskaya, located southeast of Rostov.

4.3. Flood exposure results of the 10% dam failure event

The calculated total size of the inundated area was 3 005 km^2, from which 94 km^2 was considered to be built up (See "Figure 19." and "Table 7."). The flood propagation results of the 10% dam failure simulation were similar to the results of the 5% event. The same characteristics could be observed in the dynamics of water spread, such as the uniform decrease of water velocities towards downstream and the generally high level of hazard (See "Table 7."). The total size of the areas with very low and moderate hazard dropped (they were typically classified into a higher category), while the total size of highly hazardous areas increased by approximately 21.5 km^2. These changes were mostly observed in the upper part of the 2D model area, upstream from the mouth of the Donets River. Regarding the exposure of built up areas, the most significant changes were the increase of the exposed area in Letniy Sad and Nikolaevskaya settlements, as well as the flooding of the previously unaffected Ryabichev, Yasyarev, Zadono-Kagal'nitskaya, Malomechetnyi, Vislyi settlements (See "Figure 20."). The magnitude of the effect of backwater also rose significantly in the case of both of the two most important tributaries. On the Donets, the effect of the flood wave could be detected for a length of 18.3 km upstream from the mouth, while on the Manych backwater was experienced up to the Ploretarsk Dam.

Table 7.: The total size of built-up areas according to the different hazard categories for the 10% dam failure simulation

Hazard Index	Hazard classification	Total area (km^2)
1	Very low	12.30
2	Low	17.89
3	Moderate	10.32
4	High	53.82
Total		94.33

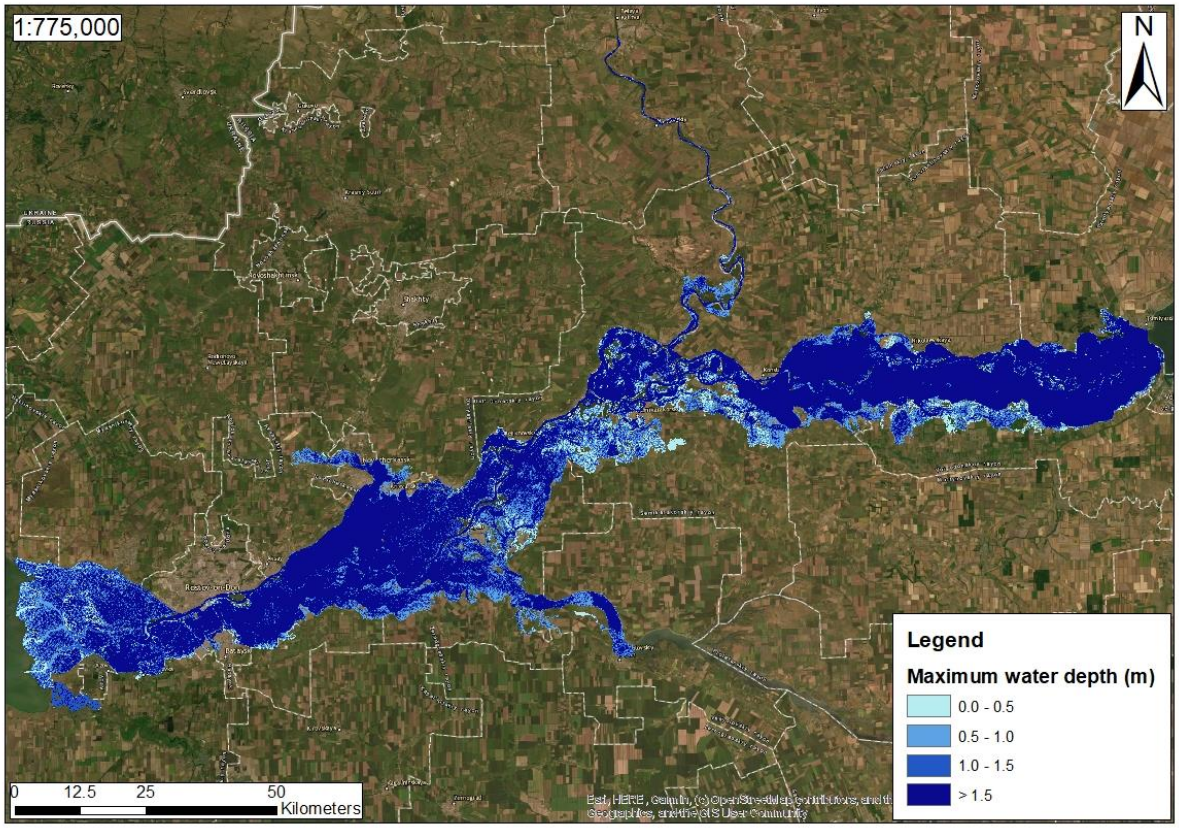

Figure 19.: Maximum water depth results of the 10% dam failure simulation

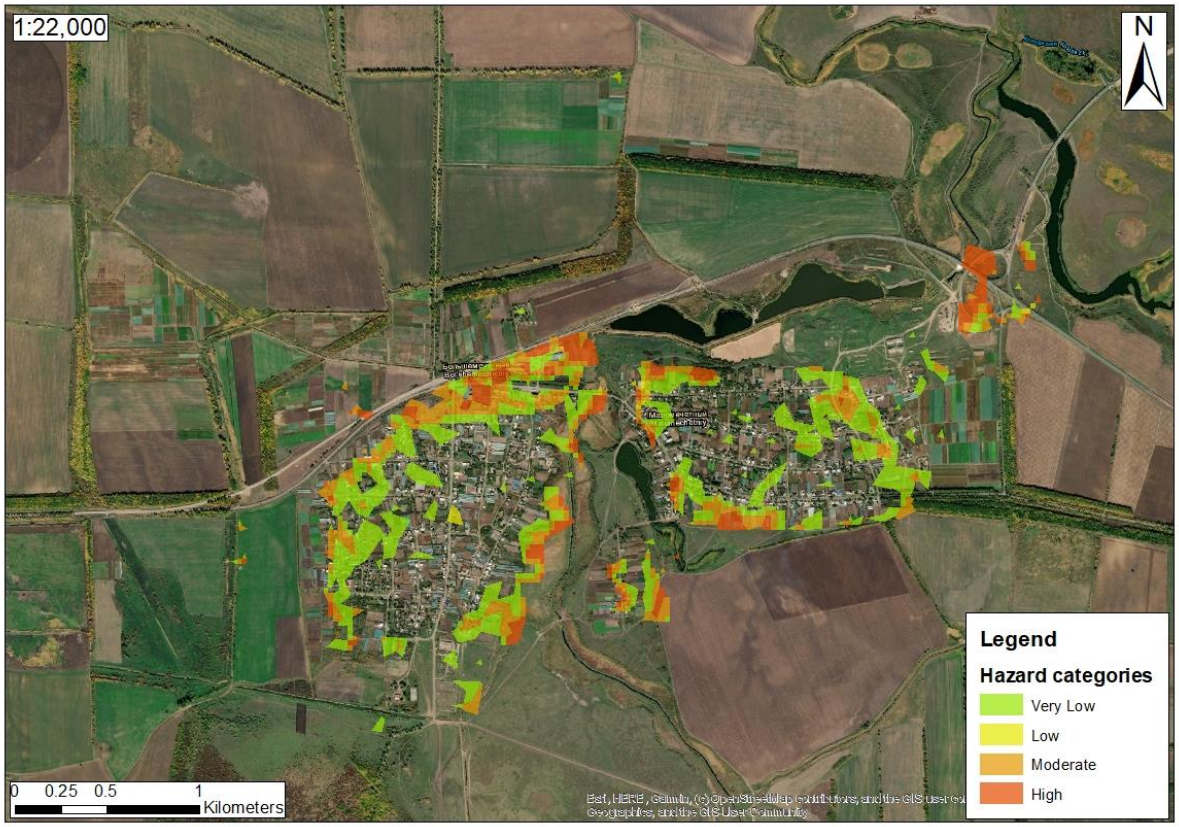

Figure 20.: Increased flood hazards around Malomechetnyi. In the case of the 5% dam failure simulation these areas were not covered by inundation

4.4. Flood exposure results of the 25% dam failure event

The results of the 25% failure simulation indicate that in the event of a disaster of this magnitude, 3 979 km^2 would be submerged, which is 41% of the entire floodplain (See "Figure 21."). In 86% of the flooded area, the maximum water depth would exceed 1 m, which is also the threshold value for the high hazard category. In the event of a 25% dam failure, the level of destruction could approach that caused by an event similar to the historic flood of 1917. The size of the total flooded built up area is about 170 km^2, which is much larger than what was measured in previous dam break scenarios (See "Table 8."). The number of affected settlements continued to increase (Ryabichev, Kholodnyi, Bolishovskaya, Morozov, Dubentsovskaya, Pirozhok, Titov etc..) mainly on the left side of the river, as well as the flood hazard in the settlements that had also been flooded in previous scenarios (See "Figure 22."). The inundation

patterns in terms of water depth and velocity changes were similar to the other dam failure simulations.

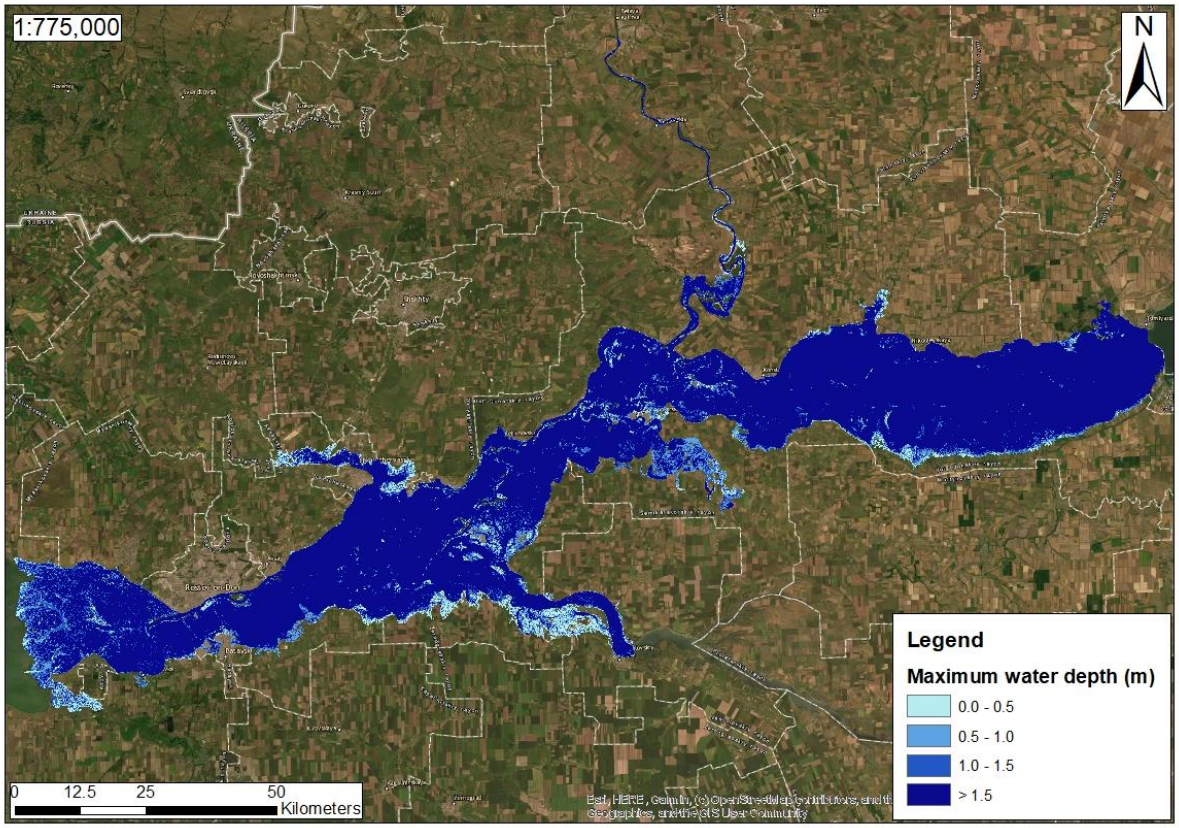

Figure 21.: Maximum water depth results of the 25% dam failure simulation

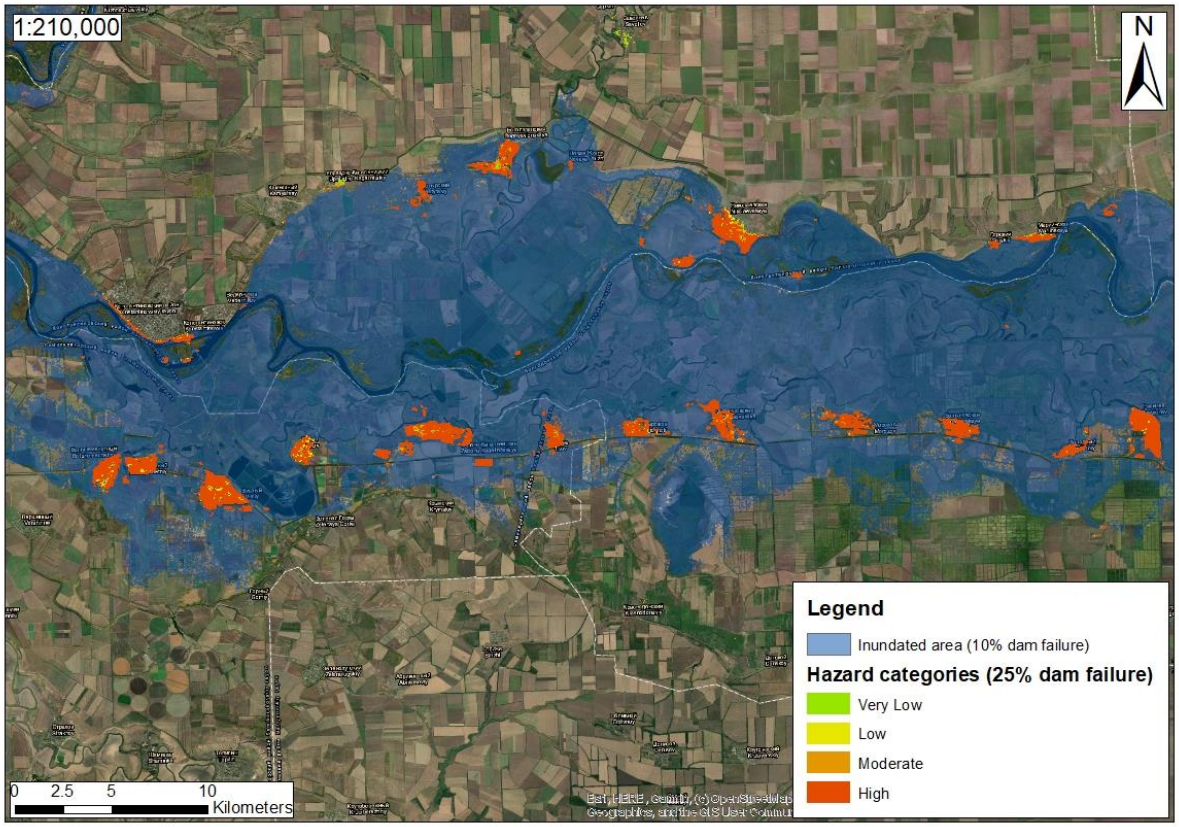

Figure 22.: Changes in flooded built up areas compared to the 10% dam failure simulation.

Table 8.: The total size of built-up areas according to the different hazard categories for the 25% dam failure simulation

Hazard Index	Hazard classification	Total area (km^2)
1	Very low	16.15
2	Low	15.71
3	Moderate	18.04
4	High	119.83
Total		169.73

4.5. Comparison of the flood exposure results

Table 9. summarizes the results of the inundation extent, water depth, water velocity, and hazard categories. According to the data presented in the table, it can be concluded that the largest inundation coverage and maximum and average water depth were experienced in the case of the 1917 historical flood scenario. Under today's land use conditions, such an event

could endanger the lives of tens of thousands of people. In terms of average and maximum water velocities, the same event shows less extreme values compared to the other scenarios. As a result of a possible dam break, the velocity of the spread of flooding in the upstream section can reach 54 m/s in some areas, and with the exception of the 5% event, the average water velocity is also higher than for the 1917 simulation. As a result of the high water velocity, water on the streets could more easily sweep away cars or cause significant damage to buildings and other valuable infrastructure. The hazard category percentage distribution data show that, in all scenarios, the high hazards of flooding dominate both for the complete inundation and for built-up areas. After studying the table, it can be said that high hazards are mostly caused by the great water depths. The average water depth was higher than the 1.5 m threshold value in all scenarios.

After studying the comprehensive GIS data tables, an examination of the differences in the extent of floodings was also carried out (See “Figure 23.”). In the case of all four scenarios, the immediate surroundings of the riverbed, almost the entire area of the Don delta, and the area close to the mouths of the inflowing streams were submerged. Increasing flood extent could be observed on the left side of the upstream floodplain, along the Donets at Nizhnekundriuchenskaya, along the Reka-Sal channel, near the Manych River at Svaboda, nearby the Reka-Tuzlov channel and around Ol'ginskaya located southwest of Rostov-On-Don.

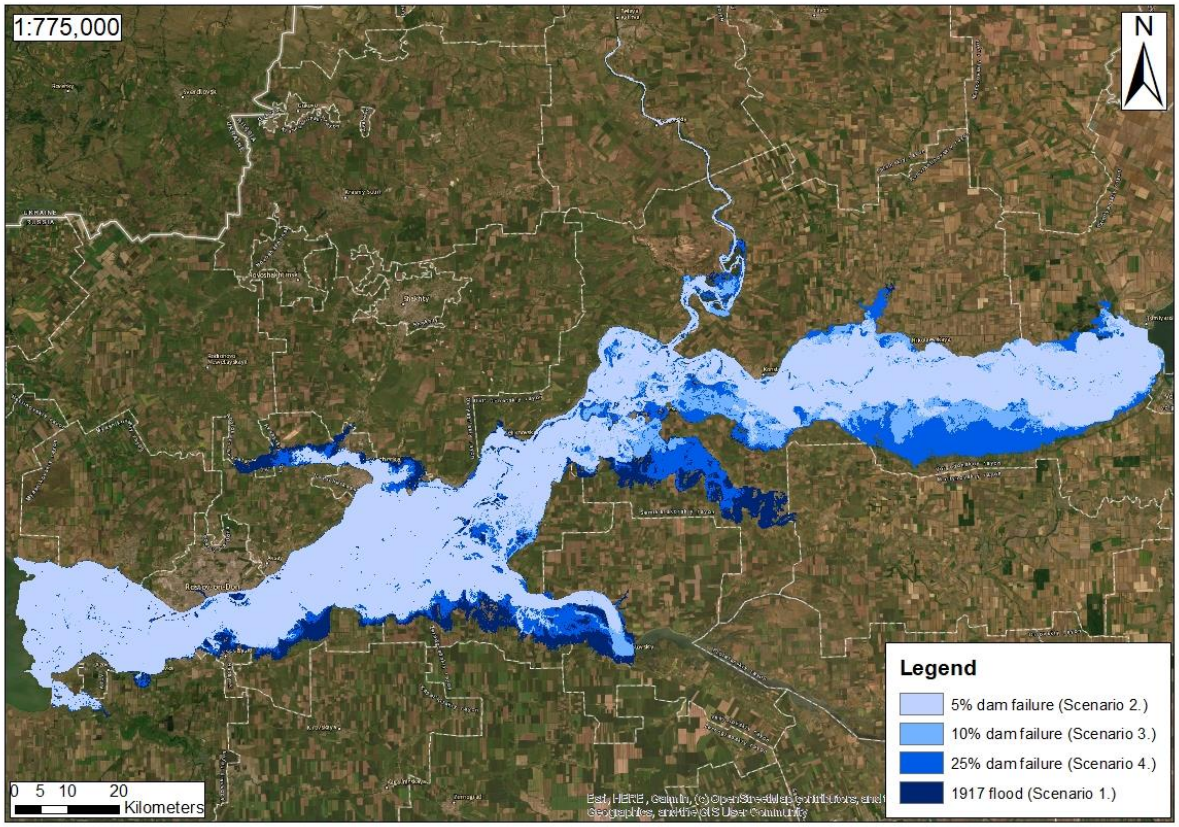

Figure 23.: Differences in flood extent among the 4 scenarios

Table 9.: Summary table of the inundation extent, maximum water discharge, water depth, water velocity, and hazard category results

Total inundation area	Name	Maximum river discharge (m^3/s)	Total inundation (km^2)	Water depth (m)		Water velocity (m/s)		Hazard category (%)			
				Maximum	Average	Maximum	Average	Very low	Low	Moderate	High
Scenario 1.	1917 historical flood	14436	4339.08	27.21	5.08	14.11	0.16	3.47	2.43	4.45	89.65
Scenario 2.	5% dam failure	16609	2525.83	19.74	2.34	54.22	0.13	11.19	7.77	16.54	64.50
Scenario 3.	10% dam failure	33218	3005.37	20.25	3.03	54.39	0.17	5.85	10.20	8.60	75.35
Scenario 4.	25% dam failure	83045	3978.88	22.44	4.57	54.87	0.24	3.82	3.63	6.25	86.30
Inundation of built up areas	**Name**	**Maximum river discharge (m^3/s)**	**Total inundation (km^2)**	**Water depth (m)**		**Water velocity (m/s)**		**Hazard category (%)**			
				Maximum	Average	Maximum	Average	Very low	Low	Moderate	High
Scenario 1.	1917 historical flood	14436	184.98	12.14	3.25	4.63	0.11	7.11	6.34	8.14	78.42
Scenario 2.	5% dam failure	16609	45.05	8.82	1.72	4.48	0.09	21.46	13.25	18.33	64.96
Scenario 3.	10% dam failure	33218	64.77	9.07	2.20	4.74	0.12	13.22	19.66	10.93	56.19
Scenario 4.	25% dam failure	83045	131.86	9.55	3.23	6.91	0.17	9.70	9.61	10.73	69.96

5. Discussion

The effects of climate change, urbanization are rapidly changing the basic functioning and characteristics of the world's riverine water systems. In order to facilitate the adaptation of local water management strategies and flood protection plans to environmental changes, it is necessary that the related data be digitized with the help of related information and communication technology. This digitization covers data storage, performing the required hydrological calculations and visualizing the results. The study identified three essential related technologies, remote sensing, GIS and hydraulic modeling, and presented their potential uses through the Lower Don River case study. The inundation results indicated that the built up areas in the Lower Don River floodplain are highly vulnerable to large water depths in case of a dam failure or an extreme flood wave triggered by climate change.

By looking at the results, it can be concluded that the software used were proved suitable for fast and efficient flood hazard mapping. The result tables and maps of the case study support the importance of proper maintenance and optimal adjustment of the operation settings of the Tsimlyansk Dam in order to prevent a destructive flood event similar to the those modeled on the Lower Don River floodplain. Based on the rapid spread of the flooding and the extensive built up area submerged, it may be justified to develop an appropriate communication and evacuation strategy in the settlements, which were affected to ensure public security. The development of flood resilience of the local population is key to efficient damage mitigation.

It is important to note that it was beyond the scope of this study to address the question of local flood protection (emergency dikes, mobile dikes, etc.). These temporary defenses can greatly influence the extent of the actual flooding. Ideally, in the case of destructive flooding events similar to the modeled scenarios, the responsible authorities quickly set up temporary protection lines with the help of firefighters, law enforcement agencies, and volunteers, thus

controlling the spread of the flood. The effectiveness of the defense largely depends on the flood arrival time and the cooperative ability of those involved in the protection procedure.

During the implementation of the hazard mapping methodology described in the study, several unexpected obstacles were encountered that had a decisive impact on the modeling results. The most significant of these limitations appeared during the methodological step of data collection. Considering that the Lower Don River basin is a data sparse area from a geospatial point of view, unfortunately, the fundamental modeling data were not of good quality in all cases. The accuracy of inundation mapping could have been greatly improved by the use of a higher resolution digital terrain model, the burning of accurate river cross section data into the DTM, more precisely defined flow hydrographs, and the validation of the final results based on real inundation maps.

Due to the 30 m resolution of the global SRTM digital elevation model, which contains several local errors, some areas may have been flooded that are not at hazard in reality. These errors are considered most critical regarding the affected built-up areas close to the riverbed. Using a higher resolution terrain data would probably have resulted in smaller flood extents, but these data are currently extremely expensive for such a large target area.

The burning of the river's bathymetry into the terrain based on relevant cross section data would have been important for two reasons. On the one hand, it would have been possible to identify the exact time step when the water exceeds the banks in a given place, and therefore would have been possible to better examine the flood arrival time of the settlements along the river. On the other hand, the inundation would also have changed slightly, as the carrying capacity of the riverbed would have been the same as in reality. Thus as much water would have flowed down in the riverbed as the Don carries in real life.

In the case of dam failure simulations, the setting of the volume-depth curve of the Tsimlyansk reservoir as the inflow boundary condition for the Don River would have been a more accurate approach. However, for this, the bathymetry data of the reservoir would have been inevitable, that unfortunately was not available. The applied flow hydrographs were based on the assumption that the given quantity of water flows down the Lower Don River in the time period of 24 hours, but in most cases, this is not compatible with the consequences of a real dam failure.

Another obstacle in high precision modeling was the lack of real inundation maps for the validation of the final results. With the help of these maps, temporary protection lines could have been identified and local inaccuracies resulting from the relatively poor resolution terrain data could have been corrected.

Further editing of the geometry of the 2D model by reducing the size of the calculation cells could have facilitated more accurate flood modeling. Unfortunately, this was not possible due to the size of the target area. In the case of HEC-RAS 2D models, the total cell count should not exceed 500 000 because such a complex geometry may result in calculation errors and significant prolongation of simulation times.

Further research and modeling is required to mitigate the effects caused by the above mentioned technical limitations. The current drastic results could be refined by using higher quality data. Thus it would be possible to define more precisely the built up areas affected by high flood hazards. Additionally, it may be important to regularly investigate the static condition of the Tsimlyansk Dam and to place a great emphasis on optimizing its operation settings. To sustain a safe environment on the downstream side of the dam is just as essential as satisfying the other environmental and social demands on the water system.

6. Conclusion

In respect of the main research question, it was found that modern remote sensing, GIS and hydraulic modeling software and tools could be used effectively to investigate flood exposure in a specific target area, as the results of the Lower Don River case study also support. These technologies provide the opportunity to build and manage complex geospatial databases, quickly perform the related hydraulic calculations, and visualize the results on a map that facilitates easy understanding. It is important to note that the introduced technologies are developing at a fast pace in recent decades, so a regular suitability review of the presented software and methodology is highly recommended.

The sub-research questions related to the case study were answered based on water depth and water velocity data generated by HEC-RAS 2D hydraulic models. The results showed that for all modeled flood scenarios, the involvement of the built up area is relatively high, which can be explained by the rapid urbanization process experienced on the Lower Don River floodplain. As a result of the rapid urban sprawl, floods similar to those modeled would threaten the safety of tens of thousands of people. In terms of the magnitude of the flood hazard, it can be said for all scenarios that both in the case of the total inundation and the inundation of built up areas high flood hazards dominated, which is mostly due to the extreme water depths. The largest inundation and water depths were produced by the 1917 historical flood simulation. The average water depth exceeded the 1.5 m threshold value in all scenarios. In terms of water velocity, the results of dam failure events indicated the most extreme values. The high water velocity results observed close to the dam ($v > 50$ m/s) could cause significant damage to the affected infrastructure, even in the case of a relatively small water depth. The flooding results were greatly influenced by the quality of the available geospatial and hydrological data and the fact that the effect of local protection lines were not taken into account in the modelling process.

Despite the presented limitations, it can be said that the safety of the built up areas of the Lower Don River floodplain largely depends on the water retention capacity of the Tsimlyansk Dam. Preserving the appropriate static condition of the dam and adapting its retention capacity to the increased water pressure due to climate change is a key issue in terms of flood control.

7. References

Aldrian, Edvin. 2021. “Indonesia’s Capital Jakarta Is Sinking. Here’s How to Stop This.” The Conversation. November 11, 2021. http://theconversation.com/indonesias-capital-jakarta-is-sinking-heres-how-to-stop-this-170269.

Australian Government, Bureau of Meteorology. 2022. “Understanding Floods.” corporateName=Bureau of Meteorology. 2022. http://www.bom.gov.au/australia/flood/knowledge-centre/understanding.shtml.

Ban, Yifang, ed. 2016. *Multitemporal Remote Sensing*. Vol. 20. Remote Sensing and Digital Image Processing. Cham: Springer International Publishing. https://doi.org/10.1007/978-3-319-47037-5.

Bashfield, A, and A Keim. 2011. “Continent-Wide DEM Creation for the European Union,” 4.

Bendixen, Mette, Jim Best, Chris Hackney, and Lars Lønsmann Iversen. 2019. “Time Is Running out for Sand.” *Nature* 571 (7763): 29–31. https://doi.org/10.1038/d41586-019-02042-4.

Bergh, B.P.J. van den. 2000. “Management of Spatial Data in Multidisciplinary Projects.” https://www.isprs.org/proceedings/XXXIII/congress/part4/1107_XXXIII-part4.pdf.

Brody, Samuel, Russell Blessing, Antonia Sebastian, and Philip Bedient. 2014. “Examining the Impact of Land Use/Land Cover Characteristics on Flood Losses.” *Journal of Environmental Planning and Management* 57 (8): 1252–65. https://doi.org/10.1080/09640568.2013.802228.

Brown, Chrisopher F., Steven P. Brumby, Brookie Guzder-Williams, Tanya Birch, Samantha Brooks, and Joseph Mazzariello. 2022. “Dynamic World, Near Real-Time Global 10 m Land Use Land Cover Mapping | Scientific Data.” June 2022. https://www.nature.com/articles/s41597-022-01307-4.

Cocheci, Matei. 2014. “Environmental Impact Assessment of Urban Sprawl in the Braşov.” 2014. https://paperzz.com/doc/8647436/environmental-impact-assessment-of-urban-sprawl-in-the-br...

Cook, John, Naomi Oreskes, Peter T. Doran, William R. L. Anderegg, Bart Verheggen, Ed W. Maibach, J. Stuart Carlton, et al. 2016. “Consensus on Consensus: A Synthesis of Consensus Estimates on Human-Caused Global Warming.” *Environmental Research Letters* 11 (4): 048002. https://doi.org/10.1088/1748-9326/11/4/048002.

Davies, Richard. 2022. “Indonesia – Floods and Landslides Leave 4 Dead, Thousands Affected – FloodList.” 2022. https://floodlist.com/asia/indonesia-floods-landslides-may-2022.

DHI. 2021. “MIKE 11 - A Modelling System for Rivers and Channels - Reference Manual.” https://manuals.mikepoweredbydhi.help/2021/Water_Resources/Mike_11_ref.pdf.

Djebou, Dagbegnon C. Sohoulande, and Vijay P. Singh. 2016. “Impact of Climate Change on Precipitation Patterns: A Comparative Approach - Sohoulande Djebou - 2016 - International Journal of Climatology - Wiley Online Library.” January 21, 2016. https://rmets.onlinelibrary.wiley.com/doi/full/10.1002/joc.4578?casa_token=K1T8-wbp8HAAAAAA%3A6S9rFa5JCWv_hZmMNcWsHyyHL2q8ivXa7VFrraPQYX8ol8qxvNxq8gXObudBy_uV4bmKlwzai1ts_Hw.

Domeneghetti, Alessio. 2016. “On the Use of SRTM and Altimetry Data for Flood Modeling in Data-Sparse Regions.” *Water Resources Research* 52 (4): 2901–18. https://doi.org/10.1002/2015WR017967.

Dore, Mohammed H. I. 2005. “Climate Change and Changes in Global Precipitation Patterns: What Do We Know?” *Environment International* 31 (8): 1167–81. https://doi.org/10.1016/j.envint.2005.03.004.
Dzhamalov, R.G., N.L. Frolova, and M.B. Kireeva. 2013. “Current Changes in River Water Regime in the Don River Basin | SpringerLink.” November 7, 2013. https://link.springer.com/article/10.1134/S0097807813060043.
Elachi, Charles, and Jakob J. van Zyl. 2021. *Introduction to the Physics and Techniques of Remote Sensing*. John Wiley & Sons.
EM-DAT. 2022. “Classification | EM-DAT.” March 20, 2022. https://www.emdat.be/classification.
Ettema, R. 2000. *Hydraulic Modeling*. American Society of Civil Engineers. https://doi.org/10.1061/9780784404157.
European Commission. 2007. “Flood Risk Management - Water - Environment - European Commission.” 2007. https://ec.europa.eu/environment/water/flood_risk/.
European Environment Agency. 2022. “Digital Terrain Model — European Environment Agency.” Term. 2022. https://www.eea.europa.eu/help/glossary/eea-glossary/digital-terrain-model.
European Space Agency. 2008. “Earth from Space: Russia’s Tsimlyansk Reservoir.” 2008. https://www.esa.int/Applications/Observing_the_Earth/Earth_from_Space_Russia_s_Tsimlyansk_Reservoir.
Gavrilov, Aleksandr Mikhaylovich, and Philip P. Micklin. 2022. “Don River | River, Russia | Britannica.” 2022. https://www.britannica.com/place/Don-River.
Gelfan, A. N., E. M. Gusev, A. S. Kalugin, I. N. Krylenko, Yu. G. Motovilov, O. N. Nasonova, T. D. Millionshchikova, and N. L. Frolova. 2022. “Runoff of Russian Rivers under Current and Projected Climate Change: A Review 2. Climate Change Impact on the Water Regime of Russian Rivers in the XXI Century.” *Water Resources* 49 (3): 351–65. https://doi.org/10.1134/S0097807822030058.
Georgievsky, M.V., and O.F. Golovanov. 2019. “Forecasting changes in river water resources of Russian Federation based on CMIP5 runoff data.”
GISGeography. 2016. “DEM, DSM & DTM Differences - A Look at Elevation Models in GIS.” GIS Geography. March 9, 2016. https://gisgeography.com/dem-dsm-dtm-differences/.
Gunasekera, Rashmin. 2004. “Use of GIS for Environmental Impact Assessment: An Interdisciplinary Approach.” *Interdisciplinary Science Reviews* 29 (1): 37–48. https://doi.org/10.1179/030801804225012473.
Harris County Flood Control District. 2019. “HEC-RAS 2D Modelin Guidelines for Site Development.” https://rashms.com/wp-content/uploads/2021/02/HCFCD-2D-Modeling-Guidelines-2019.pdf.
Hawkins, E., D. Frame, L. Harrington, M. Joshi, A. King, M. Rojas, and R. Sutton. 2020. “Observed Emergence of the Climate Change Signal: From the Familiar to the Unknown.” *Geophysical Research Letters* 47 (6): e2019GL086259. https://doi.org/10.1029/2019GL086259.
Hoque, Roxana, Daichi Nakayama, Hiroshi Matsuyama, and Jun Matsumoto. 2011. “Flood Monitoring, Mapping and Assessing Capabilities Using RADARSAT Remote Sensing, GIS and Ground Data for Bangladesh.” *Natural Hazards* 57 (2): 525–48. https://doi.org/10.1007/s11069-010-9638-y.
Hydrologic Engineering Center. 2016. “HEC-RAS - River Analysis System - Reference Manual.” https://www.hec.usace.army.mil/software/hec-ras/documentation/HEC-RAS%205.0%20Reference%20Manual.pdf.

———. 2022. “1D vs. 2D Hydraulic Modeling.” 2022. https://www.hec.usace.army.mil/confluence/rasdocs/r2dum/latest/steady-vs-unsteady-flow-and-1d-vs-2d-modeling/1d-vs-2d-hydraulic-modeling.
Icyimpaye, Gisele, Chérifa Abdelbaki, and Khaldoon A. Mourad. 2022. “Hydrological and Hydraulic Model for Flood Forecasting in Rwanda.” *Modeling Earth Systems and Environment* 8 (1): 1179–89. https://doi.org/10.1007/s40808-021-01146-z.
Kaźmierczak, Aleksandra, and Gina Cavan. 2011. “Surface Water Flooding Risk to Urban Communities: Analysis of Vulnerability, Hazard and Exposure.” *Landscape and Urban Planning* 103 (2): 185–97. https://doi.org/10.1016/j.landurbplan.2011.07.008.
Khetsuriani, E.D., V.P. Kostyukov, and E.G. Ugrovatova. 2016. “Hydrological Studies on the River Don around the Alexandrovsky OSV Water-Intake Facilities.” *Procedia Engineering* 150: 2358–63. https://doi.org/10.1016/j.proeng.2016.07.326.
Kreibich, Heidi, Philip Bubeck, Mathijs Van Vliet, and Hans De Moel. 2015. “A Review of Damage-Reducing Measures to Manage Fluvial Flood Risks in a Changing Climate.” *Mitigation and Adaptation Strategies for Global Change* 20 (6): 967–89. https://doi.org/10.1007/s11027-014-9629-5.
Kvasha, Anastasia. 2014. “Assessing Flood Risk for Urban Areas in the Lower Don River Using GIS and Remote Sensing. Master of Science Theis, Central European University, Budapest.”
Lagutov, Viktor. 2022. The hydrological regime of the Lower Don River basin. Central European University.
Lagutov, Viktor, Nikolay Dronin, and Andrei Kirilenko. 2010. “Environmental Security in Watersheds: The Sea of Azov -Chapter 3 - Climate Change, Water and Agriculture in the Azov Sea Basin.” The NATO Science for Peace and Security Programme.
Land4Flood. 2017. “LAND4FLOOD Project – Land4Flood.” 2017. https://www.land4flood.eu/land4flood-project/.
Lee, Kristen. 2022. “HEC-RAS Simulation of the India Dam Break.” Engineering Archive. https://doi.org/10.31224/2211.
Li, Jian, and David P. Roy. 2017. “A Global Analysis of Sentinel-2A, Sentinel-2B and Landsat-8 Data Revisit Intervals and Implications for Terrestrial Monitoring.” *Remote Sensing* 9 (9): 902. https://doi.org/10.3390/rs9090902.
MacOdrum Libary. 2022. “Digital Elevation Model (DEM) Formats | MacOdrum Library.” January 19, 2022. https://library.carleton.ca/guides/help/dem-formats.
Maguire, D. J. 1991. “An Overview and Definition of GIS.” http://lidecc.cs.uns.edu.ar/~nbb/ccm/downloads/Literatura/OVERVIEW%20AND%20DEFINITION%20OF%20GIS.pdf.
Matishov G.G., Chikin A.L., Berdnikov S.V., and Sheverdyaev I.V. 2013. “The extreme flood in the don river delta, March 23-24, 2013, and determining factors - ProQuest.” 2013. https://www.proquest.com/openview/6d1bcdc702ab418fa9d7eb972ef97168/1?pq-origsite=gscholar&cbl=54876.
Mayo, Talea L., and Ning Lin. 2022. “Climate Change Impacts to the Coastal Flood Hazard in the Northeastern United States - ScienceDirect.” 2022. https://www.sciencedirect.com/science/article/pii/S2212094722000378.
Mirza, M. Monirul Qader. 2003. “Climate Change and Extreme Weather Events: Can Developing Countries Adapt?” *Climate Policy* 3 (3): 233–48. https://doi.org/10.3763/cpol.2003.0330.
Morvan, Hervé, Donald Knight, Nigel Wright, Xiaonan Tang, and Amanda Crossley. 2008. “The Concept of Roughness in Fluvial Hydraulics and Its Formulation in 1D, 2D and

3D Numerical Simulation Models." *Journal of Hydraulic Research* 46 (2): 191–208. https://doi.org/10.1080/00221686.2008.9521855.
Mourato, Sandra, Paulo Fernandez, Fábio Marques, Alfredo Rocha, and Luísa Pereira. 2021. "An Interactive Web-GIS Fluvial Flood Forecast and Alert System in Operation in Portugal." *International Journal of Disaster Risk Reduction* 58 (May): 102201. https://doi.org/10.1016/j.ijdrr.2021.102201.
Nair, Saranya Chandramohanan, and Ashwini Mirajkar. 2021. "Land Use-Land Cover Anomalies and Groundwater Pattern with Climate Change for Western Vidarbha: A Case Study." *Arabian Journal of Geosciences* 14 (6): 452. https://doi.org/10.1007/s12517-021-06823-y.
NASA. 2021. "Research Shows More People Living in Floodplains." Text.Article. NASA Earth Observatory. September 27, 2021. https://earthobservatory.nasa.gov/images/148866/research-shows-more-people-living-in-floodplains.
———. 2022. "Climate Change Evidence: How Do We Know?" Climate Change: Vital Signs of the Planet. 2022. https://climate.nasa.gov/evidence.
NOAA. 2022. "National Weather Service Automated Flood Warning Systems." March 20, 2022. https://water.weather.gov/afws/afws_about.php.
NPA. 2022. "ПРАВИЛА ИСПОЛЬЗОВАНИЯ ВОДНЫХ РЕСУРСОВ ЦИМЛЯНСКОГО ВОДОХРАНИЛИЩА - [RULES FOR THE USE OF WATER RESOURCES OF THE TSIMLYANSK RESERVOIR]." 2022. https://bazanpa.ru/rosvodresursy-prikaz-n114-ot02062016-h2838733/pravila/?view_type=doc_source.
OCHA. 2022. "2021 Disasters in Numbers - World | ReliefWeb." 2022. https://reliefweb.int/report/world/2021-disasters-numbers.
Parrott, R., and F.P. Stutz. 1991. "Urban GIS Applications." https://scholar.google.com/scholar?hl=hu&as_sdt=0%2C5&q=gis+application+urban+planning+&btnG=.
Rector, Rebecca Kraft. 2016. *The Early River Valley Civilizations*. The Rosen Publishing Group, Inc.
Rosenzweig, Bernice R., Lauren McPhillips, Heejun Chang, Chingwen Cheng, Claire Welty, Marissa Matsler, David Iwaniec, and Cliff I. Davidson. 2018. "Pluvial Flood Risk and Opportunities for Resilience." *WIREs Water* 5 (6): e1302. https://doi.org/10.1002/wat2.1302.
ROSSTAT. 2013. "Regions of Russia. Socio-economic Indicators. Moscow."
Rosvodresursy. 2013. "Tsimlyansk Reservoir water resources and regulations."
Ruchin, Alexander, Oleg Artaev, Elvira Sharapova, Oleg Ermakov, Renat Zamaletdinov, Vjacheslav Korzikov, Ivan Bashinsky, et al. 2020. "Occurrence of the Amphibians in the Volga, Don River Basins and Adjacent Territories (Russia): Research in 1996-2020." *Biodiversity Data Journal* 8 (December): e61378. https://doi.org/10.3897/BDJ.8.e61378.
Schumann, G., P. Matgen, M. E. J. Cutler, A. Black, L. Hoffmann, and L. Pfister. 2008. "Comparison of Remotely Sensed Water Stages from LiDAR, Topographic Contours and SRTM." *ISPRS Journal of Photogrammetry and Remote Sensing* 63 (3): 283–96. https://doi.org/10.1016/j.isprsjprs.2007.09.004.
Shamsi, Sam U. 2022. "GIS Applications in Floodplain Management." 2022. https://proceedings.esri.com/library/userconf/proc02/pap0490/p0490.htm.
Short, Nicholas M. 2003. "A Remote Sensing Tutorial" 2: 5.
Sikka, A. K., B. Bapuji Rao, and V. U. M. Rao. 2016. "Agricultural Disaster Management and Contingency Planning to Meet the Challenges of Extreme Weather Events." *MAUSAM* 67 (1): 155–68. https://doi.org/10.54302/mausam.v67i1.1173.

Stern, Nicholas Herbert. 2006. *The Economics of Climate Change: The Stern Review*. Cambridge University Press.
Tamiru, Habtamu, and Megersa O. Dinka. 2021. "Application of ANN and HEC-RAS Model for Flood Inundation Mapping in Lower Baro Akobo River Basin, Ethiopia." *Journal of Hydrology: Regional Studies* 36 (August): 100855. https://doi.org/10.1016/j.ejrh.2021.100855.
Tellman, B., J. A. Sullivan, C. Kuhn, A. J. Kettner, C. S. Doyle, G. R. Brakenridge, T. A. Erickson, and D. A. Slayback. 2021. "Satellite Imaging Reveals Increased Proportion of Population Exposed to Floods." *Nature* 596 (7870): 80–86. https://doi.org/10.1038/s41586-021-03695-w.
Thieken, Annegret H., Philip Bubeck, Anna Heidenreich, Jennifer von Keyserlingk, Lisa Dillenardt, and Antje Otto. 2022. "Performance of the Flood Warning System in Germany in July 2021 – Insights from Affected Residents." *EGUsphere*, April, 1–26. https://doi.org/10.5194/egusphere-2022-244.
Timofeyeva, V.V. 2008. "Lower Don channel morphodynamics and its changes under the influence of anthropogenic factors. MSU Faculty of Geography."
Union of Concerned Scientists. 2022. "Average Life Expectancy of Select Infrastructure Types and Potential Climate-Related Vulnerabilities." https://www.ucsusa.org/sites/default/files/attach/gw-smart-infrastructure-table-life-expectancy.pdf.
United Nations University. 2021. "Ageing Dams Pose Growing Threat - United Nations University." January 22, 2021. https://unu.edu/media-relations/releases/ageing-dams-pose-growing-threat.html.
UNOOSA. 2022. "Recommended Practice: Flood Mapping and Damage Assessment Using Sentinel-2 (S2) Optical Data | UN-SPIDER Knowledge Portal." 2022. https://www.un-spider.org/advisory-support/recommended-practices/recommended-practice-flood-mapping-and-damage-assessment.
Vashist, Komal, and K. K. Singh. 2021. "Minimisation of Overestimation of River Flows in 1D- Hydrodynamic Modeling." Preprint. In Review. https://doi.org/10.21203/rs.3.rs-654833/v1.
Vazhacharickal, Prem, Anakha Raju, and Geethu Thomas. 2018. *Role of Information Technology in Flood Disaster Management in Kerala: A Brief Overview*.
Wandinger, Ulla. 2005. "Introduction to Lidar." In *Lidar: Range-Resolved Optical Remote Sensing of the Atmosphere*, edited by Claus Weitkamp, 1–18. Springer Series in Optical Sciences. New York, NY: Springer. https://doi.org/10.1007/0-387-25101-4_1.
WHO. 2022. "Floods." 2022. https://www.who.int/health-topics/floods.
Woodruff, Johnatan D., Jennifer L. Irish, and Suzana J. Camargo. 2013. "Coastal Flooding by Tropical Cyclones and Sea-Level Rise | Nature." December 4, 2013. https://www.nature.com/articles/nature12855.
World Bank. 2022. "Russian Federation | Data." 2022. https://data.worldbank.org/country/RU.
WWF. 2008. "Russia and Neighboring Countries: Environmental, Economic and Social Impacts of Climate Change." WWF Russia. 2008. https://wwf.ru/en/resources/publications/booklets/russia-and-neighboring-countries-environmental-economic-and-social-impacts-of-climate-change/.
Yan, Kun, Giuliano Di Baldassarre, and Dimitri P. Solomatine. 2013. "Exploring the Potential of SRTM Topographic Data for Flood Inundation Modelling under Uncertainty | Journal of Hydroinformatics | IWA Publishing." 2013. https://iwaponline.com/jh/article/15/3/849/3303/Exploring-the-potential-of-SRTM-topographic-data.

Yihdego, Yohannes. 2016. “Evaluation of Flow Reduction Due to Hydraulic Barrier Engineering Structure: Case of Urban Area Flood, Contamination and Pollution Risk Assessment.” *Geotechnical and Geological Engineering* 34 (5): 1643–54. https://doi.org/10.1007/s10706-016-0071-1.

Zhang, Y. -K., and K. E. Schilling. 2006. “Effects of Land Cover on Water Table, Soil Moisture, Evapotranspiration, and Groundwater Recharge: A Field Observation and Analysis.” *Journal of Hydrology* 319 (1): 328–38. https://doi.org/10.1016/j.jhydrol.2005.06.044.

Zope, P. E., T. I. Eldho, and V. Jothiprakash. 2017. “Hydrological Impacts of Land Use–Land Cover Change and Detention Basins on Urban Flood Hazard: A Case Study of Poisar River Basin, Mumbai, India.” *Natural Hazards* 87 (3): 1267–83. https://doi.org/10.1007/s11069-017-2816-4.